JOURNAL
of the
OPTICAL SOCIETY
OF AMERICA

VOLUME 22
No. 12

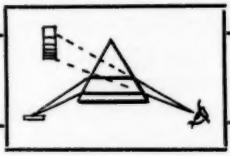

DECEMBER
1932

AN ANALYTICAL TREATMENT OF THE LONGITUDINAL HOROPTER; ITS MEASUREMENT AND APPLICATION TO RELATED PHENOMENA, ESPECIALLY TO THE RELATIVE SIZE AND SHAPE OF THE OCULAR IMAGES*

By Kenneth N. Ogle

[Department of Research in Physiological Optics, Dartmouth Medical School, Hanover, N. H. Received June 2, 1932]

TABLE OF CONTENTS

PAGE

I. Preface 666

II. Introduction 667

A. General 667
B. Analytical procedure 671

III. The Symmetrical Longitudinal Horopter 672

A. Fundamental equation 673
B. The trace of the symmetrical longitudinal horopter 675
C. The practical analytical equation 678
D. The theoretical variation in shape of trace with change of fixation-distance 679

* Acknowledgment is made to an anonymous donor for a subvention partially to defray cost of publication of this article. Editor.

IV. GENERAL LONGITUDINAL HOROPTER EQUATION—THE SKEW LONGITUDINAL HOROPTER 680
A. THE FUNDAMENTAL EQUATION 680
B. THE PRACTICAL ANALYTICAL EQUATION 683
V. PROCEDURE FOR APPLICATION TO EXPERIMENTAL DATA 684
A. ISO-MAGNIFICATION CURVES AND TRANSFORMATION GRAPHS 684
B. APPLICATION TO EMPIRICAL HOROPTER 690
VI. APPLICATION OF ANALYSIS TO FIXATION DISPARITY AND THE POSITION OF THE TRUE LONGITUDINAL HOROPTER IN SPACE 694
VII. APPLICATION OF PRINCIPLES TO OCULAR IMAGES 702
A. DISTORTION OF THE INDIVIDUAL OCULAR IMAGES AND PARTITION EXPERIMENTS 702
B. THE RELATION OF THE SIZE AND SHAPE OF THE OCULAR IMAGES TO THE PROJECTION OF RETINAL POINTS 708
VIII. THE APPLICATION OF THE ANALYSIS TO THE APPARENT ROTATION AND THE DISTORTION OF THE VISUAL FIELD ... 711
A. ROTATION OF THE HOROPTER 711
B. DISTORTION OF THE HOROPTER 713
IX. THE APPLICATION OF THE ANALYSIS TO THE LONGITUDINAL MAGNITUDE OF THE FUSIONAL AREAS (PANUM'S CIRCLES OF SENSATION) 715
X. THE CIRCLE APPROXIMATION OF THE LONGITUDINAL HOROPTER 720
XI. THE PRECISION OF MEASUREMENTS 722
A. ERROR IN FIXATION DISTANCES 723
B. ERROR IN INTERPUPILLARY DISTANCE 724
C. ERROR DUE TO SLIGHT ROTATION OF THE HEAD 725
D. ERROR DUE TO LATERAL DISPLACEMENT OF THE HEAD .. 727

I. PREFACE

This laboratory has been primarily interested of late in problems involving the relative size and shape of the ocular images in the two eyes, the horopter and corresponding retinal points. The results of its work in these fields are being presented in the following papers:

A. Ames, Jr., G. H. Gliddon and K. N. Ogle, *Size and Shape of Ocular Images. I. Methods of Determination and Physiologic Significance.* Archiv. of Ophth., *7*, p. 576; 1932.

E. H. Carleton, M.D. and L. F. Madigan, *Size and Shape of Ocular Images. II. Clinical Significance.* Archiv. of Ophth., *7*, p. 720; 1932.

A. Ames, Jr., and K. N. Ogle, *Size and Shape of Ocular Images. III. Visual Sensitivity to Differences in the Relative Size of the Ocular Images of the Two Eyes.* Archiv. of Ophth., *7*, p. 904; 1932.

A. Ames, Jr., K. N. Ogle and G. H. Gliddon, *Corresponding Retinal Points, the Horopter and the Size and Shape of the Ocular Images.* J.O.S.A., *22*, pp. 538, 575; 1932.

The nature of these subjects requires the use of a certain amount of mathematics to insure not only a correct experimental procedure, but also to provide a means for a fruitful interpretation of the experimental results. Since the mathematics required is somewhat beyond the grasp of the average reader, it seemed advisable to present the mathematical theory and technique that had been developed and has been used in the work described above, in a separate paper. As in all such research, the experimental work, the mathematical technique and the general understanding of the subject develop simultaneously, each being dependent upon the others. The particular analytical technique presented here developed with the general research work of the laboratory, and embodies many specific ideas and suggestions contributed by individual members of the department and especially those by Professor A. Ames, Jr.

II. INTRODUCTION

A. GENERAL

The determination of the relative size and shape of the ocular images[1] is intimately associated with the problem of the corresponding retinal points of the two eyes. The spatial counterparts of these corresponding retinal elements constitute the horopter, hence the determination of the horopter is a means for studying the relative size and shape of the ocular images. In general the horopter is a more inclusive concept than size and shape of the ocular images and the problem will be approached through its analytical description. Before entering into such an analysis of the horopter, a brief description, together with a short history of the physical and physiological facts upon which the horopter depends,[2] will be given.

The horopter exists only with binocular vision when the two images

[1] The term ocular image is used here to describe the impression formed in the higher brain centers through the vision of one eye. It is determined not only by the properties of the dioptric image that is formed on the retina of the eye, but also by the modifications imposed upon that image by the anatomical properties and physiological processes by which this optical image is carried to the higher brain centers.

[2] Refer to the papers listed above and the references mentioned there.

of the fixation object which are formed in the retinas of the two eyes, are fused. Point images to fuse, must fall on sensitive elements of the two retinas which innervate the same cortical regions of the brain. For schematic representation let N_1 and N_2 (Fig. 1) be the optical centers of the two eyes which are fixated upon the point F. The images of F will then fall upon the foveas of the retinas at retinal points f_1 and f_2 and will be assumed to fuse. Consider now any other point P in the visual field, the images of which fall on retinal elements at p_1 and p_2. If these elements innervate the same *regions* in the visual cortex they will fuse and will appear as single. If these two retinal points are connected directly

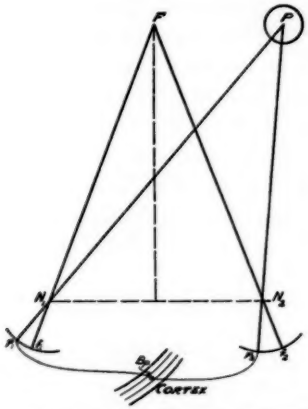

FIG. 1. *Diagrammatic illustration of the concept of corresponding points.*

to the same *center* of those regions in the cortex, they are said to be corresponding points. When the eyes are fixated, the images of any object point in space that fall on corresponding points will appear to have the same subjective direction as seen monocularly by each eye. This follows from the hypothesis that any pair of corresponding points when stimulated, innervate only one cortical center with which center a specific subjective sense of direction is associated. In general, to every retinal element in one eye there is a corresponding retinal element in the other. With binocular vision each pair of corresponding retinal elements will have two counterparts; one a point in external space and the other, a center in the visual cortex associated with a specific subjective sense of direction. The horopter is defined as "the totality of those points in external space, whose images for a given position of the eyes, fall on corresponding points in both eyes." (Helmholtz.) Thus for

a given point of fixation the horopter is a surface in space which is the loci of points determined by the intersection of visual or optical projection lines proceeding outward from corresponding retinal points of the two eyes.

Since experiment has shown that the point P may vary slightly in position and fusion still be maintained, there must be small areas of secondary connection either in the retinas or in the tracts themselves, within which the ocular images from the two eyes will be fused. The centers of these areas may be thought of as being the "corresponding points." If the images of P (Fig. 1) fall within such areas but not on corresponding elements they are said to be disparate. In the longitudinal meridians disparity aids the binocular sense of stereoscopic relief.

The general mathematical nature of the horopter as a two space correspondence problem was investigated independently by Helmholtz[3] and Hering[4] about 1862, and subsequently by others, although special features of it had been emphasized somewhat earlier. These treatments fail to give an analytical basis on which experimental data can be examined. The total surface and its behavior under certain conditions may be complex. Usually particular portions which are simpler to find experimentally, are considered. The nature of these will depend upon the general properties of the surface and the method of measurement.

E. Hering assumed, when the eyes were symmetrically converged, that objects which appear to lie in the fixation frontal plane (i.e., the plane through the point of fixation perpendicular to the visual and median planes) did actually lie on the horopter. He accordingly devised apparatus for experimentally determining what is known as the longitudinal horopter. His method consists in setting a series of vertical threads or plumb lines, properly shielded, in an apparent frontal plane, while the central one is used for the fixation object. The longitudinal horopter so determined depends only upon the longitudinal[5] components of the direction values associated with corresponding retinal points. The horopter so determined is represented by a curve in the visual plane. The latter is therefore a close approximation to the central horizontal meridian of the total horopter surface. From geometric considerations Vieth and J. Müller first showed this curve to be a circle which passes through the centers of the eyes and the point of fixation.

The experimental data obtained with Hering's method by many ex-

[3] Helmholtz, *Physiological Optics*, Eng. Trans., *III*, p. 460 ff.

[4] Beiträge zur Physiologie, *III*, Leipzig, 1863, pp. 171–224; also *IV*, 1864.

[5] Using Hering's biaxial nodo-centric division of the retina.

perimenters, including Tschermak and Fischer,[6] have indicated that the longitudinal horopter lies nearer to the fixation frontal plane than to the Vieth-Müller circle. In subsequent experiments, Fischer used Tschermak's "binocular nonius method" to check the positions of black threads on a white background when adjusted for the apparent frontal plane. He considered these experiments to substantiate Hering's findings and criterion for determining the horopter. The deviation of the longitudinal horopter from the Vieth-Müller circle has been known as the Hering-Hillebrand horopter deviation and has been considered in relation to the results of the Kundt partition experiments.[7] These would indicate effectively that the separation of the retinal elements increases toward the nasal sides of the retinas.

It was from this line of investigation that Hillebrand[8] concluded that the apparent positions of corresponding retinal points remained fixed, i.e., stable. Some evidence had been found that the shape of the longitudinal horopter varied in a definite manner when the point of fixation receded from the observer as would be required by a fixed but apparently unequal separation of retinal elements across the retinas. In general Hillebrand considered that for near vision the longitudinal horopter was concave toward the observer, and that as the point moved farther away the horopter became less and less concave and at a certain distance actually lay in the frontal plane.[9] From this point, as the fixation receded farther, the horopter trace became increasingly convex to the observer. Certain subsequent experimenters[10] have qualitatively confirmed this behavior.

Although the stability of the pattern of optically projected directional values of retinal elements under all adjustments of the eyes would appear doubtful, and although recent experimental work has shown that the objective determination of corresponding retinal points by the apparent frontal plane may be incorrect,[11] yet the general tendency in behavior of the longitudinal horopter as conceived by Hillebrand and others is probably true. Thus for a given normal observer there may

[6] E. P. Fischer, Pflügers Arch., *204*, p. 234; 1924.

[7] M. Frank, Pflügers Arch., *109*, p. 62; 1905.

[8] F. Hillebrand, Zeits. f. Psych. u. Physiol. d. Sinnesorg, *V*, pp. 1–60; 1893.

[9] K. vom Hofe, Graefes Arch., *117*, p. 40; 1926; and F. B. Hofmann, Graefes S. Handb. d. ges. A., 2nd. Ed., *III*, p. 414, 1920, fix the abathic distance for normal persons at about one meter.

[10] Helmholtz, among others.

[11] Ames, Ogle and Gliddon, *Corresponding Retinal Points, the Horopter, and the Size and Shape of Ocular Images*, J.O.S.A., *22*, p. 579; 1932.

exist a fixation distance (real or imaginary) for which the longitudinal horopter determined by corresponding retinal elements in the two eyes lies in the fixation frontal plane. This concept furnishes a convenient basis on which to begin an analytical development of the properties of the longitudinal horopter from a new point of view. The application of the results to experimental data, from a quantitative point of view, has been very fruitful and has provided an important basis for the study of particular horopter abnormalities, and other associated phenomena.

B. ANALYTICAL PROCEDURE

For the following development the eyes will be treated with certain simplifications. It is convenient to stipulate the existence of fixed nodal points or better, optical centers, or Tschermak's perspectival centers. This will not affect the essential considerations. Tschermak considers that the assumption of such centers does not permit valid conclusions to be drawn regarding the horopter. He states:[12]

> The mathematical comprehension and formulation of the empirical horopter certainly does constitute a tempting and an important aim. However, we cannot think of attaining it, until a formula has been determined for the regression of the schematic 'perspectival center' and until the individual asymmetry values and aberration constants have been obtained. If such factors were not included, the experiment of a mathematical formulation would have to be characterized as unproductive, especially since no empirical checking of their merits would be possible! The hitherto customary projection through a stable center, i.e., through the so-called mean nodal point or through the center of curvature of the retina (the latter according to Vieth and Müller) is no doubt unauthorized and is used here merely for reasons of tradition and demonstration. Strictly speaking, it is only admissable in the numerical comparison of the image position of contiguous external points (for instance, in the color and time horopter) to simply contrast the nodal angles of incidence with each other.

While it is true that mathematically exact conclusions regarding the horopter cannot be known unless the individual asymmetry values and aberration constants are known, yet valuable information can be obtained without such knowledge. As will be shown, any point on the trace of the longitudinal horopter as determined experimentally by any criterion, can be described in terms of the relative differences in the longitudinal angles subtended by the point under consideration and the fixation point, to fixed centers in each eye. In view of the greater distance of the horopter trace from the eyes compared with the interocular distance, small changes in the position of the fixed centers have only a second order effect on the relative differences between the longitudinal angles.[13] The magnitude of the effect is in general below the experi-

[12] Transl. from Bethe's Hand. d. Norm. u. Pathol. Physiol., *12*, (2), p. 897; 1930.

[13] Reference 11, p. 542.

mental error save for very near fixation distances. While some latitude is possible in the selection of the position of such centers, it is desirable that their positions represent as nearly as possible the physical facts. Thus the centers in each eye chosen to be the vertices of longitudinal angles should approximate what in an ideal system would be the anterior nodal points. Then the longitudinal angles more nearly specify angles between the optical projections of retinal elements. Tschermak has shown that the perspectival centers of the eyes through which rays determine the parts of the confusion circles on the retina where there is maximum light intensity are near the mean nodal points.[14] For this reason these points have been chosen as the vertices of longitudinal angles with which to describe the longitudinal horopter.

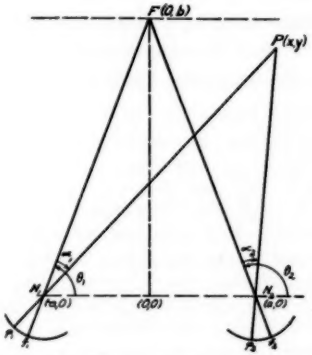

FIG. 2. *Geometric diagram for the analytic procedure.*

With the stipulation of mean nodal points as described above, the analytical development is as follows.

III. THE SYMMETRICAL LONGITUDINAL HOROPTER

In Fig. 2, let N_1 and N_2 represent the mean nodal points (optical centers) of the left and right eyes at points $(-a, 0)$ and $(a, 0)$ on a rectangular coordinate system whose origin coincides with the cyclopean projection center; i.e., the midpoint of the line connecting the mean nodal points. The distance $2a$ is then the nodal point base line. Let the point of fixation of the eyes be a distance b from the cyclopean projection center, and since, for the present, symmetrical convergence is assumed, it will be represented at coordinates $(0, b)$.

[14] Reference 12, p. 859; 1930.

For purposes of treatment, suppose θ_1 and θ_2 to be the angles included between the X axis and the fixation sight lines, measured positively counterclockwise as indicated by the arrows in the figure. Now suppose that any point $P(x, y)$ is the spatial value in the visual plane of the corresponding retinal elements p_1 and p_2, i.e., the intersection of the lines from these corresponding retinal points projected through the mean nodal points. Let the angles included between these directrices and the fixation lines be α_1 and α_2, *viz.*, the longitudinal angles to retinal elements, measured positively *clockwise*.[15] Thus, positive values of α_1 indicate angles for retinal elements on the temporal side of the left eye, while positive values for α_2 indicate angles for retinal elements on the nasal side of the right eye. Likewise, in general, positive values of α_1 and α_2 pertain to the right spatial field and negative values to the left spatial field. These angles are then of utmost importance, for it will be the relations between them that will be used to describe the shape of the trace of the longitudinal horopter, and hence the relative shape of the two ocular images, for any given convergence of the eyes.

A. THE FUNDAMENTAL EQUATION

The type of functional relation between the longitudinal angles, to any point on the trace of the longitudinal horopter can be easily found, as follows. The lines representing visual lines to $P(x, y)$ from N_1 and N_2, are given by

$$y = (x + a) \tan (\theta_1 - \alpha_1)$$

$$y = (x - a) \tan (\theta_2 - \alpha_2)$$

i.e.,

$$y = [(d - w_1)/(1 + dw_1)](x + a) \tag{1}$$

$$y = [(-d - w_2)/(1 - dw_2)](x - a) \tag{2}$$

where

$$d = \tan \theta_1 = b/a = -\tan \theta_2$$

$$w_1 = \tan \alpha_1;\ w_2 = \tan \alpha_2.$$

Assume now that there exists a distance b for a given observer for which the trace of the longitudinal horopter, whether determinable experimentally or not, is a straight line lying in the fixation frontal-parallel plane. It is required to find the relation which must exist between the angles α_1 and α_2 for that horopter. Eqs. (1) and (2) involve two sets of variables w_1 as a function of w_2, and y as a function of x. One of these sets must be known before the other can be determined.

[15] The arbitrary change in direction of these angles from that of θ_1 and θ_2 is convenient to avoid confusion, as will be evident later.

By substituting $y=b$, i.e., a straight line trace of the longitudinal horopter, the second functional relation is specified, and hence the first can be found. Hence substituting $y=b$, and eliminating x, one obtains

$$w_1w_2 - [(b/2a)w_2] + [(b/2a)w_1] = 0;$$

whence

$$1/w_1 - 1/w_2 = 2a/b. \tag{3}$$

This equation states the relation that exists between α_1 and α_2 in terms of their tangents, and thus describes points on the trace and also the *apparent* relative positions of the corresponding peripheral retinal points from the apparent position of the fixation elements of the two eyes, so that for the fixation distance b, the longitudinal horopter shall lie in the fixation frontal plane. Fortunately, it is of relatively simple form and involves the easily obtainable constants, the nodal point base line and the fixation distance in a single term. To repeat, however, the significant fact of the equation is that it states the relative distortion gradient or distribution of the optically projected longitudinal values of corresponding elements of one eye relative to that in the other, for the individual who, at a fixation distance b, sets the longitudinal horopter in the fixation frontal plane.

In general, the experimental longitudinal horopter as determined by several criteria does not lie in the fixation frontal plane, but takes a form convex or concave toward the observer. A general equation which might express the form of this curve is

$$1/w_1 - 1/w_2 = H(1 + Aw_2 + Bw_2^2 + \cdots) \tag{4}$$

where H is a constant. If the general symmetrical horopter can be described by Eq. (4) as written, it would show that for any fixation distance b, the particular shape of the trace will depend upon the value of the right-hand member. This value will be determined by the relative distribution of the projection of corresponding elements in the two eyes. Now, it is well known that the Vieth-Müller horopter circle is obtained only when the longitudinal angles of the two eyes are equal (i.e., when $w_1=w_2$) throughout the visual field. Thus, the traces of the longitudinal horopters which lie in the Vieth-Müller circle or in the frontal plane should be members of a family of curves symmetrical with respect to the median plane. These two cases could be members of a family of curves of conic sections.[16] If so, the right-hand member of

[16] This assumption that conic sections might describe the trace of the longitudinal horopter, while quite reasonable, is justified only by the results of experiment and is, accordingly, made with that in mind.

Eq. (4) will not contain any terms involving functions of w_1 and w_2 since all five conditions for a conic section will be satisfied. Between the Vieth-Müller circle and the frontal plane, the value of H would vary from zero to $2a/b$.

The fundamental equation to express the longitudinal symmetrical horopter would take the form, then,

$$1/w_1 - 1/w_2 = H \tag{5}$$

where, for a given individual, H is a constant for the fixation distance b. Before discussing the complete significance of this equation it is best to show how the shape of the trace of the horopter in the visual plane will depend upon the H.

B. THE TRACE OF THE SYMMETRICAL LONGITUDINAL HOROPTER

Now, with Eqs. (1), (2) and (5), the general space equation for conic sections as a function of the constant H can be obtained. That is, with

$$y = [(d - w_1)/(1 + dw_1)](x + a) \tag{1}$$

$$y = [(-d - w_2)/(1 - dw_2)](x - a) \tag{2}$$

$$1/w_1 - 1/w_2 = H. \tag{5}$$

By eliminating w_1 and w_2 one obtains

$$x^2\left[1 - H\frac{b}{2a}\right] + y^2\left[1 + H\frac{a}{2b}\right] - y\left[\frac{b^2 - a^2}{b} + Ha\right] - a^2 + H\frac{ab}{2} = 0 \tag{6}$$

which may be a general equation for the space coordinates of points on the trace of the longitudinal horopter for symmetrical convergence of the eyes. It would represent a horopter symmetrical with respect to the coordinate axes. The particular shape of the horopter as expressed by this equation, can be best studied by finding the family of curves it represents as the value of H varies.

If $H \equiv 0$, it is clear that $w_1 = w_2$, or $\alpha_1 = \alpha_2$, i.e., the distributions of the projections of corresponding retinal elements for each eye are equal though one is the mirrored image of the other. Eq. (6) becomes

$$x^2 + y^2 - y[(b^2 - a^2)/b] - a^2 = 0$$

or

$$x^2 + [y - (b^2 - a^2)/2b]^2 - [(b^2 + a^2)/2b]^2 = 0. \tag{7}$$

This is the equation of a circle whose center is at

$$y = (b^2 - a^2)/2b \tag{8}$$

and whose radius is $(b^2+a^2)/2b$. It is the equation of the well-known *Vieth-Müller* horopter circle. The original conception of this circle was considered to be due to equally spaced projections of retinal elements clear across the longitudinal sections of the retinas. However, the same circle will also be obtained if *any* distribution occurs in one eye so long as it is reversed identically in the other. It is to be noted that as b, the fixation distance, increases, the radius of the circle increases, approaching in the limit $\frac{1}{2}\ b$ while the center of the circle moves slightly away from the observer. Hence for a given peripheral angle in the visual field, the Vieth-Müller circle actually deviates slightly further from the frontal plane for distance vision than for near.[17]

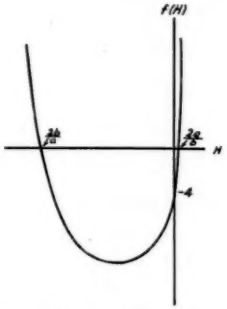

FIG. 3. *The graph of the discriminate function for the symmetrical longitudinal horopter.*

Substituting $H = 2a/b$ into Eq. (6) one obtains

$$y^2 - yb = 0;$$

whence

$$\left.\begin{aligned} y &= b \\ y &= 0 \end{aligned}\right\}. \tag{9}$$

Eqs. (9) as would be expected, represent the longitudinal horopter as parallel straight lines, one passing through the point of fixation in the frontal-parallel plane and the other passing through the two nodal points of the eyes.

The behavior of the general Eq. (6) can be easily studied by means of the discriminate, $f(H)$, *viz.*,

$$f(H) = H^2 + H[2b/a - 2a/b] - 4 \tag{10}$$

[17] Hillebrand, reference 8, p. 15.

as H assumes different values. This is the equation of a parabola (Fig. 3). The types of curves indicated as H varies, are arranged in Table 1 and shown schematically in Fig. 4.

All the curves representing the traces of different longitudinal horopters as a function of H, pass through the point of fixation F and through the two nodal points N_1 and N_2. Each of the curves will also be tangent to the fixation frontal plane at F.

TABLE 1

H	$f(H)$	Space curve of Eq. (6)
$>2a/b$	positive	A hyperbola, which passes through the point of fixation and the two nodal points
$=2a/b$	zero	Two straight lines which is a special case of the hyperbola or ellipse
$2a/b>H>0$	negative	An ellipse with major axes parallel to the x axis
$=0$	constant	The Vieth-Müller circle, being a special case of the ellipse
$0>H>-2b/a$	negative	An ellipse whose major axis coincides with the Y axis, and whose eccentricity increases until $H=-2b/a$
$=-2b/a$	zero	A parabola
$>-2b/a$	positive	A hyperbola

Thus it has been shown that the complete family of symmetrical traces may be expressed as conic sections in the variation of a single quantity H in Eq. (5). Fig. 4 illustrates the family. Beginning with the Vieth-Müller circle where H is zero, as H increases, the horopter trace becomes less and less concave to the observer, lying entirely in the frontal plane when $H=2a/b$. From this value of H, the trace is a branch of a hyperbola becoming increasingly convex to the observer. For negative values of H the trace lies entirely within the Vieth-Müller circle, the departure increasing as H increases negatively. In general, experimental data of the longitudinal horopter obtained from the apparent frontal plane method show spatial curves corresponding to positive values of H. The nearest approach to the Vieth-Müller circle was found by Tschermak and Fischer for the instantaneous horopter.

The quantity H then is a measure of the departure of a given longitudinal horopter from the Vieth-Müller circle. It is therefore a quantitative measure of the Hering-Hillebrand deviation and will, accordingly,

be denoted by H. Thus a given experimental curve, if symmetrical, can be specified by a single constant.

C. THE PRACTICAL ANALYTIC EQUATION

It is clear that Eq. (5), *viz.*,

$$1/w_1 - 1/w_2 = H$$

may be written

$$P = (w_2 - w_1)/w_1 = Hw_2. \tag{11}$$

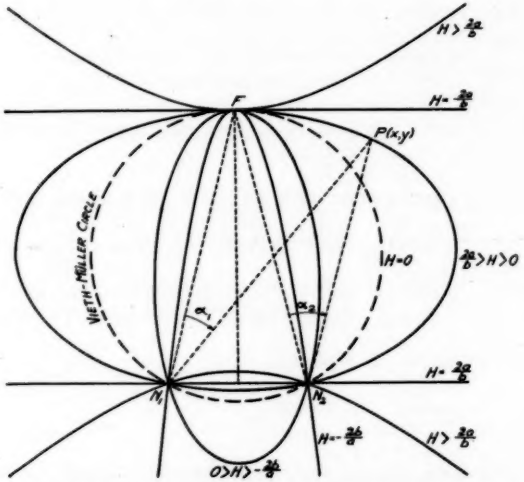

FIG. 4. *Schematic representation of the various conic sections as determined by the magnitude of H.*

When multiplied through by 100 it expresses the percentage difference in magnitude between the tangents of longitudinal angles to the two eyes determined by a point on the horopter and the fixation point. It is a linear function of the tangent of the longitudinal angle, and H the Hering-Hillebrand deviation value is the constant of proportionality. When plotted graphically the representation is a straight line,[18] the slope of which is H. This representation and its usefulness will be considered more fully later.

Since, in general, w_1 and w_2 differ only by a few percent, Eq. (11) can be written

[18] The fact that experimental data follow this linear relation, shows the adequacy of the general conic section development.

$$w_2 - w_1 = Hw^2 \text{ (approximately)} \qquad (12)$$

where w is the mean of w_1 and w_2. Assume for the sake of discussion that the apparent distribution patterns of retinal elements in the two eyes are equal, i.e., the change in magnitude of longitudinal angles for adjacent retinal elements progresses equally across the two retinas, from the nasal to the temporal sides. It is clear, from Eq. (12), that in general for positive values of w_1 and w_2, i.e., the right visual field, w_2 is greater than w_1. For negative values of w_1 and w_2, i.e., the left visual field, w_1 is greater than w_2. Hence, the apparent longitudinal angles subtended by projections from corresponding points are larger on the nasal sides of the retinas and smaller on the temporal sides. Moreover, the

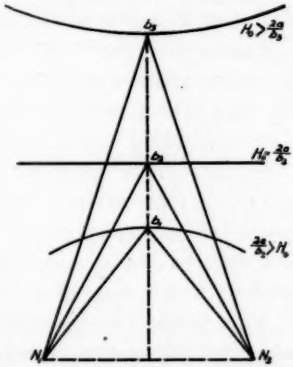

FIG. 5. *Illustration of the change in shape of the longitudinal horopter with change in fixation distance by assuming stability of corresponding retinal elements.*

apparent separation of the projections of retinal elements regularly increases from the temporal to the nasal sides of the retinas, nearly proportional to w^2. This deduction is in accordance with certain partition experiments, especially those of Kundt,[7,48] and will be considered in relation to the horopter later.

D. THE THEORETICAL VARIATION IN SHAPE OF TRACE WITH CHANGE OF FIXATION DISTANCE

Hillebrand considered that there was sufficient evidence to conclude that the *apparent* positions of the projections of corresponding points in the two eyes were fixed, i.e., stable at all fixation distances. This conclusion can be stated in terms of the above discussion by putting H a constant for a given individual for all fixation distances. Assuming the validity of this statement, we can easily examine the theoretical shape

of the horopter as the point of fixation recedes from the observer. In that case as b increases, the value of $2a/b$, which determines the value of H necessary for a frontal plane horopter, will decrease, since $2a$ remains practically constant. Consider, then, the individual whose Hering-Hillebrand deviation value is H_0. Then it is easy to find that fixation distance b_2 (Fig. 5) at which $H_0 = 2a/b_2$, for there the longitudinal horopter will lie in the frontal plane. Conceivably, b_2 might be behind the individual if H_0 were negative. For values of b less than b_2, the horopter will be concave toward the observer and for values of b greater than b_2 the horopter will be convex toward the observer, according to the curves illustrated in Fig. 4. This change in shape is in accordance with Hillebrand's theory. Recent extensive experimental data confirm his conclusion as to the variation in shape of the horopter with distance but indicate that the apparent positions of the retinal elements are not stable. This has been treated in another paper.[19]

The preceding theory has been developed to describe the relation between projections of corresponding retinal points but more explicitly the relation between the points on the trace of the longitudinal horopter. It has assumed that the horopters were symmetrical and that the images of the fixation point fall on corresponding elements. The theory, however, applies equally well to any symmetrical and regular curve anywhere in the visual plane within the region included in the field of binocular single vision. This method of description will be applied to various traces of such longitudinal horopters found experimentally by the several methods and criteria.

IV. The General Longitudinal Horopter Equation
The Skew Longitudinal Horopter

A. The fundamental equation

It might be said that the symmetrical horopter is the normal horopter. Because of its general applicability, Eq. (5) will be taken as the fundamental expression describing the trace of the longitudinal horopter in terms of the longitudinal angles of corresponding points to the two eyes. Broadly, the relation between these longitudinal angles expresses the relation between the optical projections of corresponding retinal points or the lines in the projection fans[20] and, as such, describes the relative size and shape of the ocular images in the two eyes in the horizontal meridian. Before considering this concept in particular, it is well to

[19] Reference 11, p. 597.
[20] Reference 11, p. 545.

begin with the fundamental equation and to study some of the more complex forms of the longitudinal horopter and its applications to data as additional conditions are imposed, in accordance with known related phenomena. The symmetrical horopter is one for which its axis of symmetry coincides with the median plane (Y axis). In this section a more general space horopter equation is developed and the asymmetrical case is shown to be due to an apparent inequality in the sizes of the ocular images in the two eyes.

In order to develop a consistent, and yet not a complex framework upon which such inequalities can be studied, it is necessary to proceed as follows. Suppose that for a given normal individual the separations

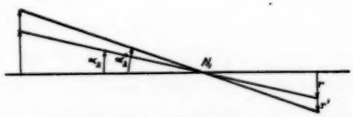

FIG. 6. *Geometric diagram for illustrating relation between separation of retinal elements and magnitude of longitudinal angles.*

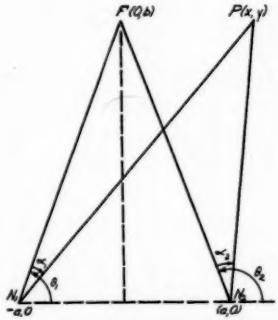

FIG. 7. *Geometric diagram for use in developing equations.*

between all the elements in the right eye are increased by a certain amount. The mean nodal point remaining fixed during this increase, the objective longitudinal angles between elements will likewise be increased. (Fig. 6.) Suppose one defines this increase by

$$\frac{r'}{r} = \frac{\tan \alpha_2'}{\tan \alpha_2} = \frac{w_2'}{w_2} = n_2 = 1 + e_2 \tag{13}$$

where $100e_2$ will represent the percent increase in the separation.[21] Now before the increase took place the horopter was symmetrical and

$$1/w_1 - 1/w_2 = H \tag{5}$$

[21] The tangent functions, instead of the actual angles themselves, are used to simplify the analysis (cf. Eq. (5)) and are consistent with the ordinary definitions of magnification for lens systems.

described adequately the relation between the longitudinal angles to corresponding points in the two eyes. Hence after the increase, the descriptive equation would become from (13)

$$1/w_1 - (1 + e_2)/w_2' = H \tag{14}$$

for an overall general increase in separation of elements by $100e_2$ percent.

It is possible now to derive the equation for the more general spatial trace for the longitudinal horopter. By substituting the analytic equivalents for the various tangents (cf. Fig. 7) and reducing, (14) becomes

$$\frac{by + a(x + a)}{b(x + a) - ay} - \frac{n_2[by - a(x - a)]}{ay + b(x - a)} = H.$$

Simplifying and collecting terms, one obtains

$$\begin{aligned} &x^2\left[1 - \frac{1}{2 + e_2} H \frac{b}{a}\right] + y^2\left[1 + \frac{1}{2 + e_2} H \frac{a}{b}\right] \\ &- xy\left[\frac{e_2}{2 + e_2} \frac{b^2 + a^2}{ab}\right] \\ &- y\left[\frac{b^2 - a^2}{b} + \frac{2}{2 + e_2} Ha\right] - a^2 + \frac{1}{2 + e_2} Hab = 0. \end{aligned} \tag{15}$$

Eq. (15) is the equation of the general conic section which passes through the three points $(-a, 0)$, $(a, 0)$ and $(0, b)$, *viz.*, the two mean nodal points of the eyes and the fixation point, and is completely specified by H and e_2, since a and b are constants. It can be shown that by proper choice of H and e_2 all possible conics through these three points are represented by it. Since an xy term is included, the conic [save when $e_2 = 0$] is not symmetrical with respect to the X, Y coordinate axes and hence is said to be skew or rotated. The degree of the skewness will depend upon the magnitude of e_2. If $e_2 = 0$ this equation reduces to Eq. (6). Also, if both H and e_2 are identically zero, the equation becomes that of the Vieth-Müller circle, *viz.*, Eq. (7). Eq. (15) then, is a more general one for the regular longitudinal horopter for symmetrical convergence. A skew longitudinal horopter for symmetrical convergence of the eyes, can be said to imply an effective magnification of the objective angles between elements in one of the eyes. The variations of Eq. (6) associated with the various forms of the conic, as H takes different values, can be applied equally well to the above general equa-

tion, the difference in the form of the conic sections resulting in their obliquity or skewness.

B. THE PRACTICAL ANALYTICAL EQUATION

Now the modified fundamental Eq. (14) from which (15) was derived, *viz.*,

$$1/w_1 - n_2/w_2' = H;\ n_2 = 1 + e_2$$

can be written

$$P = (w_2' - w_1)/w_1 = Hw_2' + e_2. \tag{16}$$

It is then in the same form as Eq. (11), which, when multiplied through by 100 expresses the percent difference in the longitudinal angles of corresponding points, in terms of those for the left eye when in addition all the longitudinal angles in the right eye are increased $100e_2$ percent over those of the left. This equation is linear, the slope being H and the intercept on the ordinate axis being e_2. The analytical interpretation of the data of the experimental longitudinal horopter will be based upon this equation. Here the characteristics of the regular longitudinal horopter are designated by two constants H, which specifies the shape of the trace, and e_2 which specifies the magnitude of the skewness or rotation of the trace about the point of fixation.

It is arbitrary to assume that the change in the separation of the projections of the corresponding retinal elements occurred in the right eye, for the rotation of a longitudinal horopter can be considered to be due to a similar change in either eye. An increase in the separation of the projections of the corresponding retinal elements in one eye would correspond to a decrease in the separation of the projections of the corresponding retinal elements in the other. If the change is assumed to take place in the left eye, by $100e_1$ percent, the fundamental equation can be written

$$n_1/w_1' - 1/w_2 = H \tag{17}$$

where $n_1 = 1 + e_1$, whence

$$P = \frac{w_2 - w_1'}{w_1'} = \frac{Hw_2}{1 + e_1} - \frac{e_1}{1 + e_1} \tag{18}$$

since for the increased separation the difference in longitudinal angles is referred to the spatial angles of the projections of retinal elements of the left eye. Substituting the analytical equivalents of the terms in

Eq. (17), as in (14), one obtains the more general space equation for the longitudinal horopter:

$$x^2\left[1-\frac{1+e_1}{2+e_1}H\frac{b}{a}\right]+y^2\left[1-\frac{1+e_1}{2+e_1}H\frac{a}{b}\right]$$
$$+xy\left[\frac{e_1}{2+e_1}\frac{b^2+a^2}{ab}\right] \tag{19}$$
$$-y\left[\frac{b^2-a^2}{b}+\frac{2(1+e_1)}{2+e_1}Ha\right]-a^2+\frac{1+e_1}{2+e_1}Hab=0.$$

This equation is consistent with (15) except in that the xy term is reversed in sign, showing that for positive values of e_1 the skewness is reversed in direction.

The relation between the decrease in the separations of one eye which will produce a given skew trace and the increase in the separation for the other to produce the same skew trace will follow from (16) and (19), *viz.*,

$$\left.\begin{aligned} e_1 &= -e_2/(1+e_2) \\ \text{and likewise} \qquad e_2 &= -e_1/(1+e_1) \end{aligned}\right\}. \tag{20}$$

V. Procedure for Application to Experimental Data

A. The Iso-Magnification Curves and Transformation Graphs

The proof that the trace of the longitudinal horopter can be represented by a conic section will be evinced only by the adequacy of the above analysis to describe experimental data. That the analysis is adequate has been demonstrated by the following method by which the data of an empirical horopter can be studied quantitatively in the general scheme formulated in Eqs. (11), (16) and (18). Specifically, each point on the trace of the longitudinal horopter or, for that matter, any other point in space, found experimentally, is to be interpreted in terms of the percent difference in the longitudinal angles subtended by each point and the fixation point to each eye. This can be done through a series of computed curves in the visual plane. Between the fixation point and every point on one of these curves longitudinal angles having a constant percentage tangent difference will be subtended at the two eyes. For convenience these curves have been termed iso-magnification curves.

Since the Vieth-Müller horopter circle is determined when the projections of corresponding points in the two eyes make equal longitudinal

angles with the elements of fixation, it is most suitable for the basic iso-magnification curve. It is clear that Eq. (15) can be used, in which H is set identically zero; *viz.*,

$$x^2 + y^2 - xy\left[\frac{e_2}{2 + e_2}\,\frac{a^2 + b^2}{ab}\right] - y\left[\frac{b^2 - a^2}{b}\right] - a^2 = 0 \qquad (21)$$

to describe a set of iso-magnification curves for the fixation distance b and nodal point base line $2a$ at which a given empirical horopter has been determined. By substituting into these equations successive values of e_2, both positive and negative, where $100e_2$ is taken as the percentage equivalent, a system of curves can be computed. All these curves pass through the point of fixation and have obliquities which

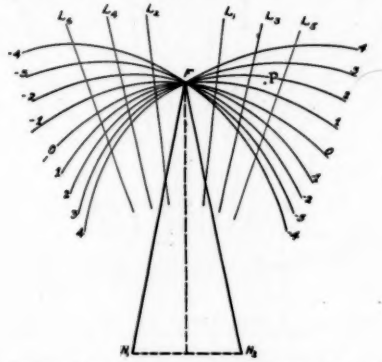

FIG. 8. *Schematic representation of iso-magnification curves for a given fixation distance.*

increase as the absolute value of e_2 increases. Fig. 8 shows such a system schematically. These curves represent the change in form of the original Vieth-Müller circle, as longitudinal angles in the right eye are progressively changed overall. By means of them any point within the visual field can be interpreted in terms of the percent difference in magnitude of longitudinal angles subtended by it at the left and right eyes. This difference may be considered as a percent magnification or diminution. Thus, should the point be on the Vieth-Müller circle the difference in longitudinal angles is zero. If the point is one as represented by P in Fig. 8, it can be said to subtend a longitudinal angle to the right eye nearly 1.50 percent larger than the corresponding longitudinal angle to the left eye.[22] By means of Eq. (20) this point can also

[22] It should be pointed out that a considerable change occurs in the space values of the iso-magnification curves at a distance compared to those for near vision. This difference takes

be said to subtend a longitudinal angle to the left eye 1.48 percent[23] smaller than the corresponding longitudinal angle to the right eye.

To understand the nature of the data of the empirical longitudinal horopter it will be necessary to describe briefly the apparatus by which the measurements were made. The present apparatus is an improvement on that used by Tschermak and collaborators, although it embodies its essential characteristics. It has the advantage of adjustment devices in a head rest by means of which the observer's eyes can be centered fairly accurately. The horopter apparatus (Fig. 9) consists of 13 channels made of steel strips mounted so that they converge to a point directly below the midpoint of the mean nodal point base line of the two eyes. The

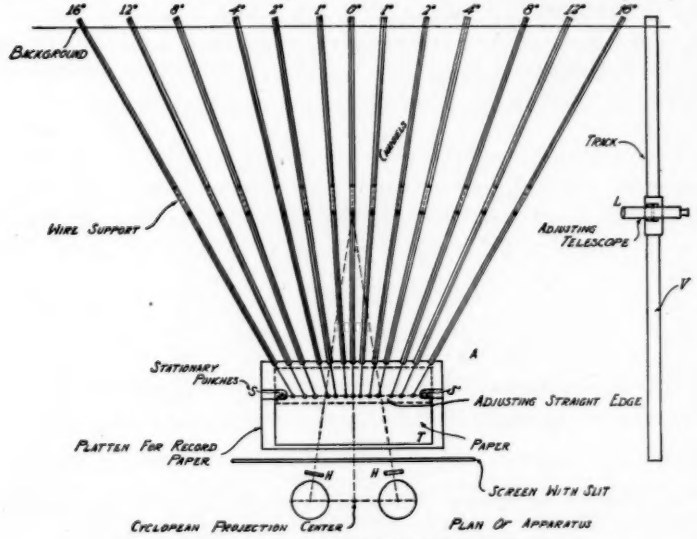

FIG. 9. *Plan of the near longitudinal horopter apparatus.*

central one lies in the median plane and the others make angles 1°, 2°, 4°, 8°, 12°, and 16° on each side of the central one. Sliding smoothly in the channels are steel strips which support vertically suitable steel drill rods (cf. threads in Hering-Tschermak apparatus). Three groups of these rods are mounted at distances of 202, 404, and 756 mm from the cyclopean center. They may be folded back out of the field of view if desired. The movement of each of the slides can be controlled by handles placed near the observer. At the end of each of the sliding strips, toward the observer, small punches are mounted which, when pushed, cause a pin prick in a

place in two ways. First the spatial separation of any two adjacent iso-magnification curves increases with the distance of fixation, almost varying directly as the square of that distance. Second, the skewness or rotation of these curves about the fixation point is very much greater for the same percent change at a distance than for near as is shown in the following section. Hence small magnifications of the ocular image of one eye will have great counterparts in space for distant vision, and will therefore be more apparent. See reference 11, p. 568.

[23] It will be shown that a considerable error can be made in the values b and a before the error in the result is above the precision of measurements.

sheet of cardboard supported on a platen beneath. By means of this arrangement a record of the position of the wires can be quickly and accurately made. Adjustment of the wires and the pins is accomplished by means of a telescope, a straight edge and stationary punches on the apparatus. The observer sees the wires of the apparatus through a long horizontal slit in a suitable screen set up so that other empirical factors will be eliminated. If the haploscopic apparatus is used simultaneously with the horopter apparatus, half-silvered plane parallel mirrors are mounted before the eyes, and with these in use corrections must be applied to all horopter data due to the displacement of the images caused by the plane parallels. Supports for ophthalmic lenses, which are always equidistant from the median plane, are mounted before the eyes on haploscopic type arms. Mounting small apertures in these supports the observer can quickly check the centering of his eyes by observing the position of the fixation point in the apertures at each eye.

The spatial points for an empirical longitudinal horopter, as determined in the laboratory, are usually recorded by the ordinate distance from the fixation frontal plane only, since the abscissa values are automatically determined by the fixed lanes of the apparatus in which the threads or wires move. If lines corresponding to the lanes of the apparatus are drawn on a large graph sheet on which the iso-magnification curves are plotted, it is a simple matter to read off the approximate percentage value for each of the points of the empirical horopter. These values may be found more accurately from computed tables, or they may be found from the transformation graphs plotted from the data of the tables. These data can be taken directly from the iso-magnification curves, or they can be computed conveniently and more precisely directly from Eq. (21) and the analytical expressions for lanes of the apparatus. Each of the lanes in the apparatus described above can be expressed by $x = my$, where $m = \tan \phi$, ϕ being the angle of the lane from the central lane. Substituting this value of x into Eq. (21), solving for e_2 and replacing e_2 by $P = [(w_2 - w_1)/w_1]$, one obtains

$$P = -2\frac{y^2(m^2+1) - Sy - a^2}{y^2(m^2+1-mG) - Sy - a^2}$$

where

$$G = (a^2 + b^2)/ab \quad \text{and} \quad S = (b^2 - a^2)/b.$$

Now if $c = (y - b)$ is the reading for a given point on the horopter measured from the fixation frontal plane, for a given lane angle ϕ, one can compute P from

$$P = -2\frac{(b+c)^2(m^2+1) - (b+c)S - a^2}{(b+c)^2[m^2+1-mG] - (b+c)S - a^2}$$

or

$$P = -2/(1-K) \tag{23}$$

TABLE 2. *Computed data for plotting iso-magnification curves and transformation graphs.*

4.94 D

Lane		Left field 16°	12°	8°	4°	2°	1°	0	Right field 1°	2°	4°	8°	12°	16°
						b = 20.0 cm								
Distance from frontal plane for percent increase of longitudinal angles of O.D. mm	0%	−14.79	− 8.42	− 3.77	−0.95	−0.24	−0.06		−0.06	−0.24	−0.95	− 3.77	− 8.42	−14.79
	3%	−19.15	−11.90	− 6.20	−2.20	−0.87	−0.38		0.25	0.40	0.35	− 1.28	− 4.82	−10.20
	8%	−26.18	−17.40	−10.00	−4.18	−1.90	−0.90		0.80	1.48	2.40	2.80	1.25	− 2.45
	−3%	−10.05	− 4.70	− 1.20	0.35	0.40	0.25		−0.38	−0.90	−2.20	− 6.26	−12.00	−19.25
	−8%	− 1.30	2.10	3.40	2.62	1.48	0.75		−0.90	−1.90	−4.40	−10.50	−17.80	−26.40

2.500 D

Lane		Left field 16°	12°	8°	4°	2°	1°	0	Right field 1°	2°	4°	8°	12°	16°
						b = 40.4 cm								
Distance from frontal plane for percent increase of longitudinal angles of O.D. mm	0%	−30.5	−17.36	− 7.78	−1.95	−0.49	−0.12		−0.12	−0.49	−1.95	− 7.78	−17.36	−30.5
	2%		−26.8	−14.3	−5.4	−2.20	−0.99		0.70	1.20	1.53	− 0.9	− 7.3	−17.7
	4%			−20.6	−8.65	−3.85	−1.85		1.60	2.98	5.0	6.1	3.0	− 4.6
	−2%	−17.5	− 7.1	− 0.8	1.6	1.30	0.79		−1.00	−2.22	−5.4	−14.5	−26.9	
	−4%	− 3.4	3.9	6.6	5.3	3.17	1.68		−1.90	−4.00	−8.9	−21.1		

TABLE 2 (*Continued*).

1.33 D

Lane		Left field 16°	12°	8°	4°	2°	1°	0	Right field 1°	2°	4°	8°	12°	16°
Distance from frontal plane for percent increase of longitudinal angles of O.D. mm	0%		−32.7	−14.63	− 3.68	−0.92	−0.23		−0.23	−0.92	− 3.68	−14.63	−32.7	
	1%			−26.45	− 9.65	−3.92	−1.73		1.22	2.20	2.45	− 2.45	−15.2	−35.8
	2.5%				−18.40	−8.40	−3.95		3.51	6.82	11.65	16.00	12.5	0.4
	−1%	−34.8	−15.0	− 2.40	2.55	2.20	1.30		−1.70	−3.99	− 9.80	−26.40		
	−2.5%	1.9	13.5	16.80	12.15	6.98	3.70		−4.05	−8.62	−18.90			

0.164 D

Lane		Left field 15°	10°	5°	0	Right field 5°	10°	15°
Distance from frontal plane for percent increase of longitudinal angles of O.D. cm	0%	− 40.9	− 18.4	− 4.7		− 4.7	− 18.4	− 40.9
	0.25%	− 73.8	− 41.7	−16.8		8.0	6.9	− 3.5
	0.50%	−103.0	− 63.1	−28.5		21.2	34.4	39.0
	1.00%	−152.9	−101.6	−50.5		49.4	97.7	145.1
	−0.25%	− 3.5	6.9	8.0		−16.8	− 41.7	− 73.8
	−0.50%	39.0	34.4	21.2		−28.5	− 63.1	−103.0
	−1.00%	145.1	97.7	49.4		−50.5	−101.6	−152.9

where

$$K = \frac{mG(b+c)^2}{(b+c)^2(m^2+1) - (b+c)S - a^2}.$$

The tables computed for plotting the iso-magnification curves and the transformation graphs for four fixation distances, are given in Table 2. The transformation graphs for the right and left visual fields for the fixation distance of 40 cm are shown in Fig. 10.

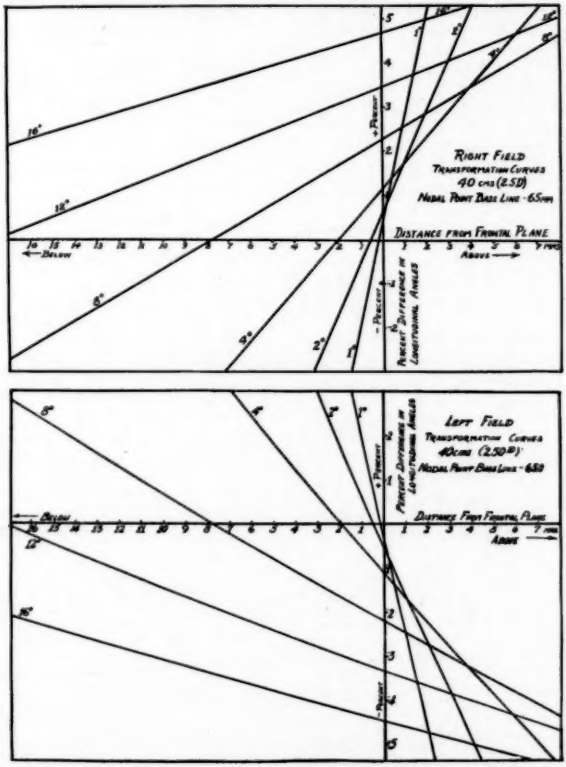

FIG. 10. *The transformation graphs for the right and left fields for the fixation distance of 40 cm.*

B. APPLICATION TO THE EMPIRICAL HOROPTER

Since a set of iso-magnification curves (or transformation curves) makes it possible to determine the percent difference value of any point on an experimental longitudinal horopter, it is convenient that experi-

mental data be so interpreted and graphed in accordance with the preceding theory. By so doing, a transformation is made from the spatial to an analytical curve, which lends itself more readily to quantitative interpretation. Since the iso-magnification curves have been arbitrarily computed, by assuming the overall changes in objective longitudinal angles to take place at the right eye, the transformed data give graphs following Eq. 16, *viz.*, in general

$$P = (w_2 - w_1)/w_1 = Hw_2 + e_2 \tag{24}$$

where $100e_2$ is percentage overall increase in longitudinal angles of the right eye. In the transformation graph the ordinates are expressed in units of percent difference $100e_2$ or $100\,P$. The abscissae are expressed in

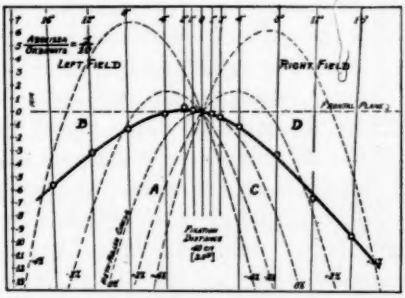

FIG. 11. *The spatial graph of a typical set of data for the apparent frontal plane (horopter).*

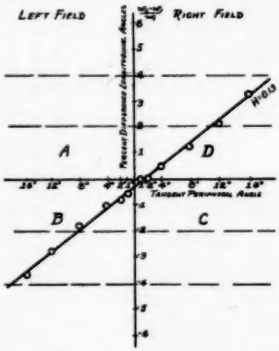

FIG. 12. *The analytical graph illustrating the data for the apparent frontal plane (horopter).*

units proportional to the tangent of the objective longitudinal angles of the right eye, i.e., w_2. Thus the axis of the abscissae will correspond to the Vieth-Müller circle and the iso-magnification curves to a series of straight lines parallel to the axis of the abscissa.

In order to make this transformation clear and to show the applicability of the method to experimental data, a typical set, Table 3, will be examined,[24] and the spatial and analytical graphs shown. In Figs. 11 and 12, the curves represent the data of the table for the apparent

[24] The data for this set were obtained by Hering's method, *viz.*, the adjustment of a series of verticle threads so that all appear to lie in a frontal plane, while a central one was used for constant fixation. The recorded data give the distance in mm that a thread in any given lane, when adjusted, lies behind (+) or in front (−) of the true fixation frontal plane. Cf., reference 11, p. 566 ff.

TABLE 3. *Apparent frontal plane (horopter) data for K.N.O. No refractive error. Fixation distance=404 mm (2.5 D). The number of settings for each lane is approximately 80.*

Lane	16°	12°	8°	4°	2°	1°	0	1°	2°	4°	8°	12°	16°
Readings mm	−5.45	−3.20	−1.35	−0.19	+0.26	+0.11		−0.14	−0.32	−1.16	−3.38	−6.56	−9.64
Mean deviation ±	1.45	0.82	0.48	0.23	0.14	0.12		0.11	0.21	0.31	0.59	0.89	1.62
Percent value from iso-mag. curves	−3.73%	−2.75%	−1.84%	−1.02%	−0.85%	−0.60%		0.00%	0.20%	0.47%	1.29%	2.15%	3.25%
Percent value of mean deviation ±	0.20%	0.16%	0.14%	0.13%	0.16%	0.34%		0.31%	0.25%	0.18%	0.18%	0.17%	0.22%

frontal plane horopter in the spatial and analytical graphs respectively. In the spatial graph, the ordinates of which are magnified ten times, three iso-magnification curves, 0 percent, ± 2.0 percent and ± 4.0 percent, have been included so that the relation between the two graphs can be more easily recognized. The quadrants of the analytical graph related to particular regions in the spatial graph are denoted by the letters A, B, C, and D, in both. Inspection of Fig. 12 shows that H, the Hering-Hillebrand deviation for this particular method, denoted by the slope of the line is about 0.13, and that there is an apparent overall change (decrease) in the longitudinal angles of the right eye of $e_2 = -0.003$, or $100e_2 = -0.3$ percent.

From extensive data[25] of which the set illustrated is typical, it is clear that the data of a regular experimental horopter are adequately specified in terms of two constants e and H by means of the transformation just presented.[26] The first, indicated by the intercept on ordinate axis, quantitatively describes any overall difference in the longitudinal angles of one eye relative to those of the other. H, the slope of the data line, describes quantitatively the degree of concavity or convexity of the horopter and therefore describes the Hering-Hillebrand deviation. The uniqueness with which the transformed data approximate straight lines in the analytical graphs would indicate, without question, that conic sections do describe empirical data at least for peripheral angles up to 16°. This deduction is further enhanced by the manner in which the above analysis describes related phenomena. The value of the transformation process and the method of study is apparent at once. The practical, and hence clinical importance, lies in the ease of detection and measurement of related phenomena and irregularities in binocular vision. In certain cases the longitudinal horopter data may not be regular and hence could not be described analytically by the constants e and H. However, the deviation of the actual data from a linear form in the analytical graph would give a measure of the irregularity and might even be expressed algebraically as a function of the peripheral angle.

The expressions developed above are readily applicable to experimental data found in the literature. For example, Helmholtz[27] ob-

[25] For further data see reference 11, p. 577 ff.

[26] Within experimental error in the field of view ordinarily used, the tangents of angles appearing in various quantitative expressions can be replaced by the angles themselves. This has been done in much of the work so as to avoid confusion for readers not accustomed to trigonometric functions. For this development, however, the functions will be used.

[27] Helmholtz, *Physiological Optics*, Eng. trans. IIIrd Ed., *III*, p. 319. See also reference 11, p. 605 ff.

tained data (Table 4) for the apparent frontal plane (horopter). By using three plumb lines, the center of which was displaced from the plane of the outer two, he found those fixation distances for which they appeared to lie in the frontal plane. The center plumb was used for constant fixation. By assuming his longitudinal horopter to be sym-

TABLE 4. *Data for the apparent frontal plane of Helmholtz and the computed value of H for each fixation distance. a=34 mm.*

Fixation distance b mm and diopters	450 2.22 D	730 1.37 D	237 4.22 D	129 7.75 D	550 1.82 D
Displacement of the central thread $y-b$	−10.5 mm	−6.0 mm	−4.2 mm	−8.1 mm	−2.0 mm
Separation of the outer threads $2x$	256 mm	256 mm	117 mm	117 mm	120 mm
Hering-Hillebrand deviation value H (Eq. 25)	0.108	0.068	0.203	0.366	0.086

metrical, all the conditions required for finding H are satisfied. Eq. (6) is used, in which H is found, *viz.*,

$$H = \frac{x^2 + y^2 - yS - a^2}{x^2b/2a - y^2a/2b + ay - ab/2} \tag{25}$$

where $S=(b^2-a^2)/b$, where x is the lateral distance from the central plumb to either of the outer threads, b is the fixation distance, $2a$ is his nodal point base line (68 mm) and $(y-b)$ is the displacement of the central plumb line from the plane of the outer plumbs. The computed results are shown in Table 4 and illustrated graphically in Fig. 13, where the abscissae express the fixation distance in diopters.[28]

VI. APPLICATION OF ANALYSIS TO FIXATION DISPARITY AND THE POSITION OF THE TRUE LONGITUDINAL HOROPTER IN SPACE[29]

The above analysis, applicable to another phenomenon that has a direct bearing upon the position of the horopter in space, will be considered now. This phenomenon, that in general an error exists in the convergence of the eyes in fixation, i.e., that there is an actual disparity at the foveas, was first mentioned by Lau[30] and examined more fully

[28] For discussion of this subject see reference 11, p. 597 ff.

[29] Ames, Gliddon and Ogle, *Size and Shape of Ocular Images. I. Methods of Determination and Physiologic Significance*, Archiv. of Ophthal., *7*, p. 576; 1932. Also reference 11, p. 586.

[30] E. Lau, Zeits. f. Sinnesphysiol., *53*, pp. 1–35; 1921.

by Hofmann[31] as a conclusion from a series of experiments. The phenomenon now called fixation disparity, was independently discovered and studied in this laboratory, having been first called "retinal slip."[32] It was then stated, "Retinal slip becomes evident when images which are in part similar and in part dissimilar are formed on the retinas of the two eyes. The similar parts fuse and appear as single. The dissimilar parts which do not fuse will appear under certain conditions to be displaced." This displacement was correlated closely with heterophoria, both in direction and magnitude, and with a slight turning of the eyes

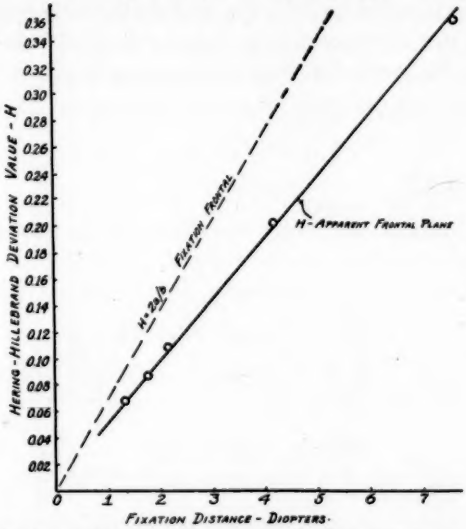

FIG. 13. *The graphical representation of the change in the Hering-Hillebrand deviation values for the apparent frontal plane from the data of Helmholtz.*

with involuntary convergence. The displacement of the dissimilar parts of the images was interpreted as a disparity resulting from a condition where the images of the fixation point in space do not fall upon corresponding retinal elements in the two eyes. These images fall within fusional areas, but angles will exist between the visual lines to the nearest pair of corresponding points[33] and the directions of fixation. The total

[31] Hofmann, Gr. S. Hand.; 2nd Ed., *3*, p. 428; 1920–1925.

[32] Ames and Gliddon, *Ocular Measurements*, Trans. section on Ophthal. of the A.M.A., p. 37 ff, 1928.

[33] Additional evidence concerning the nature of this phenomenon is to be found in the experiment on Panum's limiting case and also in the multiple partition experiments with binocular fixation. Cf. reference 11, p. 588.

fixation disparity existing at the fovea will be taken, equal in both eyes. By making this assumption the geometrical relations of the problem remain symmetrical and, accordingly, analytically simplified.

In the diagrammatic figure, Fig. 14, let σ be the $\frac{1}{2}$ total angular disparity in the two eyes, i.e., the angle between the fixation lines Ff_1 (and Ff_2) and the visual lines to the nearest pair of corresponding points Aa_1 (and Aa_2) taken in the direction indicated by the arrows. The images of F, *viz.*, f_1 and f_2 will not fall on corresponding points, but will fall within fusional areas. Each of the elements at f_1 and f_2 will have corresponding points in the opposite eye, and the intersection of the optical projections of these pairs of points gives the clue as to where the horopter will lie for the particular choice of disparate angles. Thus in the fig-

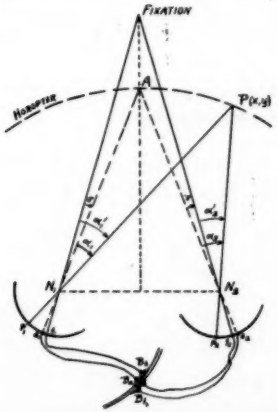

FIG. 14. *Schematic representation of the phenomenon of fixation disparity.*

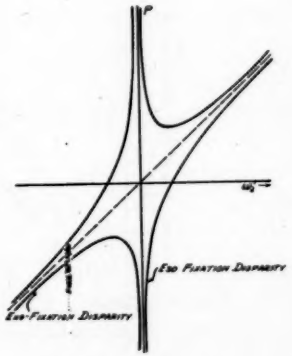

FIG. 15. *Schematic graph of the analytical graphs when fixation disparity exists.*

ure which illustrates the case of a so-called eso-fixation disparity associated with esophoria, the true horopter would lie in front of the point of fixation. It should be remembered that the disparity exists because these fixation lines do not fall on corresponding points. If the directions of the disparate angles are reversed for the case of exo-fixation disparity, associated with exophoria, the horopter will lie behind the point of fixation. These phenomena have been wholly substantiated by experiment where the true horopter is determined by means of the gridnonius horopter method. The latter is an improvement on Tschermak's nonius method.[34]

[34] Reference 29, p. 585; reference 11 p. 558.

The application of the afore-mentioned method of analysis to the problem will now be presented, together with two examples of the quantitative applicability of the theory to experimental data.

The fundamental horopter equation, Eq. (5), specified the relation between longitudinal angles to corresponding points in the two eyes, measured from the central corresponding elements of the two retinas. In the preceding development these were assumed to coincide with the fixation directions and thus no fixation disparity would exist. Now, however, since the transformation process must use iso-magnification curves determined at the fixation point, the longitudinal angles must be modified to that point of reference. Thus, if α_1' and α_2' refer to the longitudinal angles measured from the fixation lines, the longitudinal angles from the nearest pair of corresponding projection lines will be

$$\left.\begin{aligned} \alpha_1 &= \alpha_1' - \sigma \\ \alpha_2 &= \alpha_2' + \sigma \end{aligned}\right\} \tag{26}$$

where σ taken positive will relate to an exo-fixation disparity and where σ taken negative will relate to an exo-fixation disparity. Since σ is quite small compared with α, one can write for this case

$$\begin{aligned} \tan \alpha_1 &= \tan \alpha_1' - \tan \sigma \\ \tan \alpha_2 &= \tan \alpha_2' + \tan \sigma \end{aligned}$$

or

$$\left.\begin{aligned} w_1 &= w_1' - s \\ w_2 &= w_2' + s \end{aligned}\right\}. \tag{27}$$

The fundamental longitudinal horopter equation then becomes

$$1/(w_1' - s) - 1/(w_2' + s) = H. \tag{28}$$

When reduced this equation describes the type of curve that would be given by experimental data when interpreted in percent difference of longitudinal angles on the analytical graph, where $P = (w_2' - w_1')/w_1'$ is plotted against w_2', *viz.*,

$$\left[\frac{H}{1 + Hs}\right] w_2'^2 - P w_2' - \left[\frac{2s + Hs^2}{1 + Hs}\right][P + 1] = 0. \tag{29}$$

This equation specifically applies to eso-fixation disparity. To examine the case of symmetrical exo-fixation disparity it is only necessary to change the sign of s. Since the value of H, the Hering-Hillebrand horopter deviation constant, rarely has values greater than 0.3, and the value

of s, the magnitude of the symmetrical disparate angle, is in general less than ± 0.001, Eq. (29) can be written without loss of precision

$$Hw_2'^2 - Pw_2' + 2s[P + 1] = 0 \tag{30}$$

where s taken positive or negative will apply to eso- and exo-fixation disparity, respectively.

Eq. (30) is that of a hyperbola (and its conjugate when s is taken negative) (Fig. 15) having as asymptotes

$$P = (w_2' - w_1')/w_1' = Hw_2' \tag{31}$$

and

$$P = (w_2' - w_1')/w_1' = - w_2'/2s - 1. \tag{32}$$

The latter practically coincides with the ordinate axis and will be considered so. The oblique asymptote Eq. (31) has the slope of the Hering-

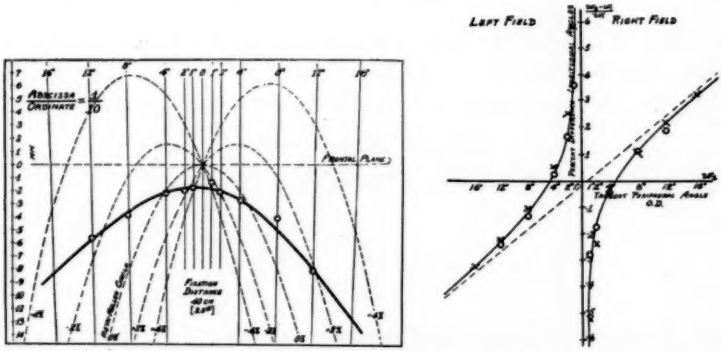

FIG. 16. *The spatial and analytical graphs of the grid-nonius (true) longitudinal horopter data of K.N.O., illustrating eso-fixation disparity.*

Hillebrand horopter deviation and hence the latter, H, can be found from data of the experimental horopter when transformed and plotted according to this scheme.

Two sets of actual data for the true longitudinal horopter obtained by the grid-nonius method are presented below in order to show the applicability of the transformation process.[35] Table 5 records the actual results of experimental determination for K.N.O. It is to be noted that the mean position of spatial points of the horopter all lie in front of the fixation object. These data, using circles, are plotted in Fig. 16. Now

[35] Taken from "*Corresponding Retinal Points*, etc." reference 11, p. 586.

TABLE 5. *Grid-nonius longitudinal horopter data of K.N.O. No refractive error. Fixation distance 404 mm (2.5 D). Eso-fixation disparity. P.D.=64 mm.*

	Left field							Right field					
Lane	16°	12°	8°	4°	2°	1°	0	1°	2°	4°	8°	12°	16°
Mean of 15 sets of readings mm	—	−5.5	−3.8	−2.3	−1.9	−1.7		−1.4	−2.1	−2.7	−4.1	−8.1	—
Mean deviation of readings mm	—	±2.8	±1.6	±0.9	±0.6	±0.4		±0.4	±0.6	±0.9	±1.8	±4.0	—
Percent values from iso-mag. curves	—	−2.38	−1.28	+0.18	+1.70	+3.60		−2.85	−1.83	−0.45	+1.07	+1.88	—
Percent values of mean deviation	—	±0.39	±0.47	±0.53	±0.68	±1.00		±1.00	±0.68	±0.50	±0.52	±0.56	—
Computed percent values from theory	−3.25	−2.20	−1.05	+0.56	+2.50	+5.80		−5.21	−2.36	−0.55	+1.04	+2.17	+3.22

from experiments with fixation disparity by K.N.O. the displacement of the unlike images was measured at many different times, with a result of 0.4 mm displacement at a distance of 400 mm. Assuming the eso-fixation disparity to be equally divided in the two eyes, one finds that the value of s would be $s=0.0005$.[36] Taking the value of H, the Hering-Hillebrand horopter deviation constant, equal to 0.125, the values of $P=(w_2'-w_1')/w_1'$ were computed for the various peripheral angles, w_2', from Eq. (31), for eso-fixation disparity, *viz.*,

$$P = (w_2' - w_1')/w_1' = (Hw_2'^2 - 2s)/(w_2' + 2s) \qquad (33)$$

and they are shown in Fig. 16, by the small crosses. Table 6 records the experimental data and also the computed values of F.D.C., a case of

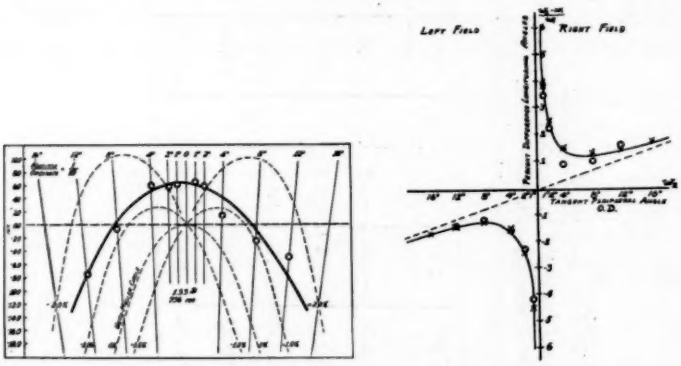

FIG. 17. *The spatial and analytical graphs of the grid-nonius (true) longitudinal horopter data of F.D.C., illustrating exo-fixation disparity.*

exo-fixation disparity. The computed values were obtained by taking $H=0.050$ and $s=-0.0004$, for a fixation distance of 756 mm. Here it will be noted that for F.D.C., an exo-fixation disparity case, the horopter lies behind the fixation point. These data are shown plotted in Fig. 17, where the circles give the points of the experimental data and the crosses give the theoretical points computed for $s=-0.0004$ ($\sigma=1.3'$).

The correlation between the theoretical and experimental data in these two examples is quite good. In general corrections may be necessary, e.g., to eliminate any overall inequality of the ocular images that may exist. Moreover, inequalities sometimes exist between the shape

[36] Recent experiment indicates that the disparity angle may exist entirely in one eye, and not be divided, as suggested above. For such a case, however, Eq. (30) is applicable, where $2s$ will be that total fixation disparity.

TABLE 6. *Grid-nonius longitudinal horopter data of F.D.C. Small astigmatic correction. Fixation distance 756 mm (1.33 D). Exo-fixation disparity. P.D.=64 mm.*

	Left field							Right field					
Lane	16°	12°	8°	4°	2°	1°	0	1°	2°	4°	8°	12°	16°
Mean of 15 sets of readings	—	−7.4	+0.5	+6.1	+5.8	+6.2		+6.5	+5.8	+1.6	−2.1	−4.9	—
Mean deviation of readings mm	—	±5.7	±6.6	±3.6	±1.0	±2.5		±2.7	±4.0	±5.6	±5.1	±5.5	—
Percent values from iso-mag. curves	—	−1.4	−1.2	−1.6	−2.2	−4.1		+4.4	+2.2	+0.9	+1.0	+1.6	—
Percent values of mean deviation	—	±0.3	±0.6	±0.5	±0.4	±1.6		±1.7	±1.4	±0.8	±0.5	±0.3	—
Computed percent values from theory	−1.7	−1.4	−1.3	−1.5	−2.4	−4.5		+4.9	+2.5	+1.5	+1.3	+1.4	+1.7

and position of the two branches of the hyperbola. This asymmetry may be due to an unequal division of the total angular fixation disparity between the two eyes.

The spatial equation expressing the longitudinal horopter in space as modified by a fixation disparity will not be developed here. For symmetrical fixation disparity it would be similar to Eq. (6), except that b as it occurs there will be replaced by an expression involving the disparity factor. It is clear, moreover, that the existence of an inequality of the ocular images of the two eyes will modify the developments of this section in complete accordance with the previous sections.

The application of the analysis presented in the foregoing pages to the determination of the horopter, to its relation to corresponding retinal points, to its relation to the apparent frontal plane horopter and to its relation to binocular vision including fixation disparity and heterophoria, has been considered in another paper from this laboratory.[37] It should be pointed out that powerful support has been presented as to the applicability of the fundamental longitudinal horopter equation to experimental data; that the latter can be specified by three constants; H, the Hering-Hillebrand horopter deviation value; e_2 the measure of any overall inequality in the size of the ocular images that may exist; and s the magnitude of the disparity factor.

VII. Application of Principles to Ocular Images

A. Distortion of the Individual Ocular Images and Partition Experiments

It has been shown that the points in the trace of the empirical longitudinal horopter can be adequately described through simple equations of conic sections. These equations depended upon a fundamental relation between the corresponding longitudinal angles subtending points on the trace and the fixation point whose vertices lie at identical centers in the two eyes. These centers in the two eyes were chosen to lie at approximate optical centers. Thus the lines determining these longitudinal angles for a given point on the trace of the horopter will approximate the optical projections of corresponding points, and as such indicate their apparent positions.

The data obtained for the longitudinal angles from the empirical longitudinal horopter give only relative magnitudes for the apparent positions of corresponding retinal elements in the two eyes. In general,

[37] Refer to papers listed in the Preface.

the fact that the longitudinal horopter does not lie on the Vieth-Müller circle, shows that a change in the relative magnitudes of the corresponding longitudinal angles exists across the visual field, and as such indicates an unbalanced distortion between the ocular images in the two eyes.[38] As shown, this effective binocular distortion can be described in a linear relation with the tangent of longitudinal angle by a single constant H, when those changes are expressed in percentage differences between the tangents of corresponding longitudinal angles. H then expresses a constant gradient in the relative ocular distortion between the two eyes. The empirical horopter shows, in general, the effective unbalanced binocular distortion is such that the apparent separation of retinal elements in the two eyes increases toward the nasal sides of the retinas.

From the horopter data alone it is impossible to determine how this distortion is divided between the two eyes. The ocular image of one eye may have a distortion reversed in direction, but the magnitude of the distortion of the other might be sufficient to give a normal longitudinal horopter in the visual field. That is, any type of distortion in one eye which is duplicated, but reversed in direction in the other, will not affect the horopter.[39] For this reason the horopter alone is inadequate for the determination of the complete distortions of each of the ocular images.[40]

The necessary additional information can be obtained by what will be called multiple partition experiments.[41] Here a series of object points are arranged so that as seen by each eye all appear equally separated directionally. The hypothesis upon which such experiments rests is the same as that for the determination of the horopter, namely that the innervation of a particular brain center gives rise to a specific subjective impression of direction. Hence a relation between the optical projections of retinal elements for one of the eyes and the associated subjective directional values must give a measure of the monocular distortion in the ocular image of that eye. Since the same directional value will result from stimulating corresponding retinal elements in the other eye, the

[38] Reference 11, p. 545 ff.

[39] This may not be strictly true in the case of certain lenses placed before the eyes.

[40] Cf. also Tschermak's "Ziehung." Bethes Handb. d. normal. u. pathol. Physiol., *12* (2) p. 907; 1930; reference 11, p. 549.

[41] As distinguished from ordinary partition experiments of dividing a line into two apparently equal segments. Cf. Bethes Handb. d. normal. u. pathol. Physiol., *12* (2) p. 846; 1930.

combined effective distortion of both eyes must correlate with the unbalanced distortion of the horopter.[42]

The means of obtaining the effective monocular distortion is to find the positions of the optical projections of retinal elements whose associated directional values are known. In this respect the absolute directional value for a particular element cannot be found since any given element cannot be tagged. However, by finding the objective projection of a number of elements whose associated directional values are equally separated, a measure of the monocular distortion can be found. Experimentally, a series of vertical threads or wires is adjusted so that they all appear equally spaced while one of them is used for a constant point of fixation. Insofar as the angular values of these objects to the eye are not equally spaced a measure of the distortion is obtained.

It would seem that the correct procedure to obtain the binocular and monocular ocular distortion is to use the type of horopter apparatus recently described by Tschermak,[43] where the angular separation of the lanes can be varied. Here the objects that are made to appear equally separated directionally are also adjusted on the horopter. When so adjusted the position of the threads provides not only the information for the unbalanced binocular distortion but the position of the threads will also give the equi-partition data for each eye, and thus provide the data for monocular ocular distortion. Apparatus is now under construction in this laboratory, for a thorough investigation of this field.

In such experiments,[44] if each of the wires were adjusted both for equal directional separation and at the same time for the true horopter, then according to the fundamental hypothesis, each of them would be associated with units of subjective impression of directional separation. Calling the central fixation[45] wire "0," the others for the right and left field will correspond to subjective units 1, 2, 3 etc. and -1, -2, -3, etc., respectively. Thus for a given subjective directional value j there will be a point on the horopter which can be described by

$$1/w_1]_j - n_2/w_2]_j = H. \tag{14}$$

Monocularly specific optical projections of a retinal element will also

[42] A. Ames and K. N. Ogle, *The Horopter and Corresponding Retinal Points*, The Annals of the Dist. Serv. Found. of Optom., *1* (1) p. 35; 1932.

[43] Tschermak, Ber. über die ges. Physiol., *61*, May, 1931.

[44] The following discussion is a more detailed account of the subject briefly described in reference 11, pp. 573, 595.

[45] If fixation disparity exists this will still be true, for the judgment of its direction will be in that of a near pair of corresponding retinal points.

be associated with a specific value of j.[46] Obviously the unit j can only be associated with an arbitrary longitudinal angle chosen as the standard directional separation. Therefore, suppose the longitudinal angles to the first wire on the horopter in the right field to be taken as this standard, and labeled w', and w'' for the O.S. and O.D., respectively, corresponding to the associated subjective unit 1. The data for the par-

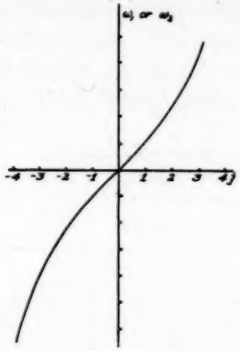

FIG. 18. *Illustration of graph when* w_1 *(or* w_2*) is plotted against the subjective directional separation unit.*

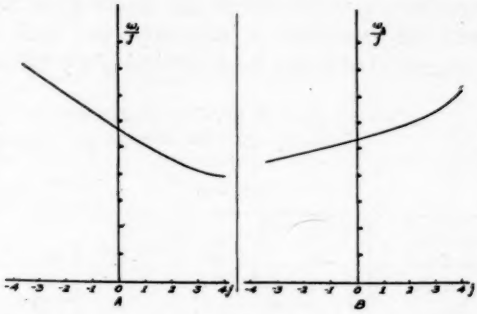

FIG. 19. *Illustration of graphs when* w_1/j *and* w_2/j *are plotted against the subjective directional separation unit.*

tition part of the experiment for each eye can be plotted in terms of the longitudinal angle and the subjective directional separation unit j, (Fig. 18) and perhaps the functions

$$\left.\begin{aligned} w_1 &= f_1(j, w') \\ w_2 &= f_2(j, w'') \end{aligned}\right\} \quad (34)$$

and

can be found.

More valuable is the graph, obtained by plotting the value w_1/j (or w_2/j) against the subjective unit j, which then expresses the objective change in longitudinal angles as j varies (Fig. 19). The same functions can be found more readily from these graphs. These functions obviously must yield the horopter equation when j is eliminated. i.e.,

$$\left.\begin{aligned} w_1 &= f_1(j, w') \\ w_2 &= f_2(j, w'') \\ 1/w_1 - n_2/w_2 &= H \\ 1/w' - n_2/w'' &= H \end{aligned}\right\} \quad (35)$$

[46] For the most complete theoretical development of the horopter probably all relations should also depend directly upon such a subjective directional unit.

must be simultaneous. Hence

$$f_2(j, w'') = n_2\left[\frac{f_1[j, w']}{1 + H[f_1(j, w'')]}\right]. \tag{36}$$

Since the new apparatus has not yet been completed there are no data by which the above can be tested. However, the theory will be applied to data previously obtained from monocular multiple partition experiments, which though not obtained correctly, may be used to illustrate the procedure. A haploscope was used, on the targets of which were mounted seven short vertical black wires, whose lateral positions

TABLE 7. *Multiple partition data. Fixation distance=400 mm—K.N.O. Haploscope apparatus. Standard space—first wire on left field.*

	Left field				Right field		
Subjective directional separation Unit=j	−3	−2	−1	0	1	2	3
Mm separation of threads from center, O.D.	−37.20	−24.23	−12.00		11.26	22.70	33.96
$w_2=\tan\alpha_2$	−0.0930	−0.0606	−0.0300		0.0281	0.0567	0.0849
α_2	−5°.314	−3°.466	−1°.718		1°.613	3°.256	4°.853
w_2/j	0.0310	0.0303	0.0300		0.0282	0.0284	0.0283
Mm separation of threads from center, O.S.	−39.82	−25.95	−12.58		12.00	24.10	36.44
Same corrected for 12.0 standard left field	−37.98	−24.75	−12.00		11.45	22.99	24.76
$w_1=\tan\alpha_1$	−0.0949	−0.0619	−0.0300		0.2862	0.0575	0.0869
α_1	−5°.424	−3°.642	−1°.719		1°.639	3°.291	4°.910
w_1/j	0.0316	0.0309	0.0300		0.0286	0.0287	0.0289

in the plane of the target could be varied by suitable screws. The central wire was used for constant fixation. With the space between the fixation wire and the first wire in the left field as the standard for the experiment, the other five wires were adjusted monocularly until all seven appeared equally spaced directionally. These data for K.N.O. are tabulated in Table 7.[47]

[47] Reference 11, p. 596.

The computed values for w_2/j and w_1/j are then plotted against j, the graphs being shown in Fig. 20, A and B. Consider, first, the data for the right eye, represented in B of Fig. 20. The exact nature of the algebraic function which would describe this is of course unknown. Here, however, a straight line serves the purpose quite well and accordingly such has been drawn in graph B. Then the expression which would describe the data would be

$$w_2/j = k_2 + h_2 j \tag{37}$$

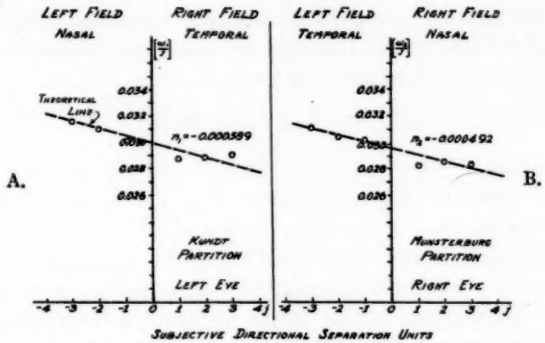

FIG. 20. *Actual graphs for the multiple partition data of K.N.O., illustrating the theoretical agreement.*

which may be considered as the result of an expansion of

$$w_2 = k_2 j/[1 - (h_2/k_2)j] \tag{38}$$

viz.,

$$= k_2 j[1 + (h_2/k_2)j + (h_2^2/k_2^2)j^2 \cdots]$$

where the terms of higher powers are neglected since h_2 is small compared to k_2 or j.

The corresponding function for w_1 which must satisfy the conditions of the longitudinal horopter will be

$$w_1 = k_1 j/[1 - (h_1/k_1)j] \tag{39}$$

for by solving (38) and (39) for j and equating, one has

$$j = \frac{1}{(k_2/w_2 + h_2/k_2)} = \frac{1}{(k_1/w_1 + h_1/k_1)}$$

whence

$$\frac{1}{w_1} - \frac{n_2}{w_2} = \frac{h_2k_1 - h_1k_2}{k_1^2k_2} = H \tag{40}$$

where

$$n_2 = k_2/k_1 = 1 + e_2. \tag{41}$$

From the graph for the right eye then one finds

$$h_2 = -0.000492 \text{ and } k_2 = 0.0295.$$

Referring to the grid-nonius graph (Fig. 16), one finds $H = 0.11$ and $e_2 = -0.10$ percent whence one can compute from Eqs. (40) and (41) that $k_1 = 0.0298$ and $h_1 = -0.000589$. Drawing the theoretical line on the graph A for the left eye Fig. 20, *viz.*,

$$w_1/j = 0.0298 - 0.000589j \tag{42}$$

one can observe to what extent the actual multiple partition data for the left eye shown by the points agree with the data of that for the right eye and that for the horopter. Such a striking agreement of these particular data is probably unusual. They serve, however, to illustrate the application of the multiple partition data to the horopter and as such add a contribution to the theory of corresponding retinal points and their physiological nature. It is to be noted that the partition data for the right eye are of the type found by Münsterburg[48] and others, indicating that the apparent separation of elements is greater toward the temporal side of the retina. On the other hand, the data for the left eye are of the type found by Kundt[48,7] and others, indicating that the apparent separation of elements is greater toward the nasal side of the retina. An excess of binocular unbalanced distortion of the Kundt type is necessary in order that H be positive, and such is found here.

The nature of the ocular images in the horizontal meridian for the two eyes can be found by this procedure.

B. RELATION OF THE SIZE AND SHAPE OF THE OCULAR IMAGE TO THE PROJECTION OF RETINAL POINTS

In any given meridian, the sum total of the optical projections of corresponding retinal elements can be thought to constitute two projection fans emerging from each eye. In the horizontal meridian the intersection of corresponding projections in these fans determines the horopter in that meridian. The arrangement of the projections for one eye in that meridian is a measure of the size and shape of the ocular image

[48] Cf. A. Tschermak, reference 12, p. 845 ff; 1930.

for that eye. For purposes of measurement these projections are referred to a common perspectival center in the eye and their magnitudes are expressed angularly from a fixed projection—the fixation line through that center. Thus the angular spacings of these projection lines define the ocular image and are dependent upon the actual anatomical distribution of the sensitive elements and the properties of the dioptric system of the eye.[49]

The size and shape of the ocular image will have an inverse relationship to the extension and shape of the projection fan. If the size of the ocular image is increased, the separation of projections in the fans is decreased.[49] This is demonstrated schematically in Fig. 21. Without the magnifying lens the object FA forms an image af on the retina. When the magnifying lens is placed before the eye, the image of AF becomes

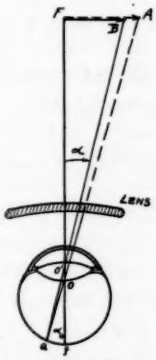

FIG. 21. *Figure to show relation between image size and the magnitude of the longitudinal angles.*

larger than af by definition. In order that the image will now fall on the same number of retinal elements as before, it is necessary to decrease the size of the object to FB. Hence the objective space angle subtending the image af will be effectively decreased. The decrease of the effective space angle here may be considered to follow from the forward shift of the optical center (nodal point) produced by the addition of the lens.

The relation between the ocular image and the magnitude of the angular separation of projection lines can be found in a simple manner as follows: In Fig. 21, before the lens is placed before the eye, let the object FA form an image af on the retina. By definition

$$af/FA = M = \text{the magnification of the image } af \text{ to the object } FA. \quad (43)$$

[49] Reference 11, p. 545 ff.

Suppose, now, the lens (which here is assumed to be of zero refractive power) whose magnification constant is specified by m, $[m=1+i]$ be placed before the eye. This magnification implicitly specifies a shift in nodal point. The image of the object FA will be increased to a new image size, say $a'f$, and one may write

$$a'f/FA = mM. \tag{44}$$

For this discussion the size of the object at F is desired which is necessary to form the same size image on the retina as that before the lens was added to the eye. Let this size be FB. Then one can write

$$af/FB = mM. \tag{45}$$

By substituting the value of af from Eq. (43), the above becomes

$$FA/FB = m = 1 + i. \tag{46}$$

Now in general, two objects whose feet are at F when referred to a common center previously chosen as the point for measuring the longitudinal angles (e.g., for the iso-magnification curves), are proportional to the tangents of the longitudinal angles and thus

$$FA/FB = w/w' = 1/(1 + e).$$

Thus

$$1/(1 + e) = 1 + i \tag{47}$$

whence

$$\left.\begin{aligned} i &= -e/(1 + e) \\ \text{and} \quad e &= -i/(1 + i) \end{aligned}\right\}. \tag{48}$$

These equations then show the relation between size of ocular image and extension of projection fan for a given angle or for overall measure. They specify the magnitudes of the apparent size as measured by the iso-magnification curves where little or no difference in distance from the eyes occurs for the position of the objects.

Frequently for simplification purposes it is convenient to specify the change in angles directly instead of that of their tangents. In doing so any overall value expressed either in terms of the tangents or the angles implies that the equivalent will depend upon the peripheral angle in question. Table 8 shows the equivalents of the tangent values for the change in size of ocular images, fans, and angle change in fans.

TABLE 8

Longitudinal angles tan. ratio $100\left(\frac{w_2-w_1}{w_1}\right)=100e$	Ocular image inverse tan. ratio $100i=\frac{-100e}{1+e}$	Longitudinal angles Angle ratio 10° $100\frac{\alpha_2-\alpha_1}{\alpha_1}\Big]$	Angle ratio 20° $100\frac{\alpha_2-\alpha_1}{\alpha_1}\Big]_{20°}$
−8.0%	8.69%	−7.83%	−7.34%
−6.0%	6.38%	−5.88%	−5.51%
−4.0%	4.17%	−3.92%	−3.68%
0.0%	0.00%	0.00%	0.00%
4.0%	−3.85%	3.92%	3.69%
6.0%	−5.66%	5.88%	5.54%
8.0%	−7.41%	7.84%	7.39%

VIII. THE APPLICATION OF THE ANALYSIS TO THE APPARENT ROTATION AND THE DISTORTION OF THE VISUAL FIELD

A. ROTATION OF THE HOROPTER

The rotation of the trace of the longitudinal horopter about the point of fixation can be interpreted as being due to an overall percent difference in the longitudinal angles to corresponding points in the two eyes, i.e., an overall percent difference in the two ocular images. Because of the wide application to depth perception and binocular vision it is important to know in terms of degrees the amount of such angular rotation of the longitudinal horopter and with it the apparent rotation of the field of single binocular vision produced by a given percent difference in the ocular images of the two eyes.[50] This can be determined from Eq. (15), *viz.*,

$$x^2\left[1-\frac{H}{2+e_2}\,\frac{b}{a}\right]-xy\left[\frac{e_2}{2+e_2}\,\frac{b^2+a^2}{ab}\right]+y^2\left[1+\frac{H}{2+e_2}\,\frac{a}{b}\right]$$
$$-y\left[\frac{b^2-a^2}{b}+\frac{2Ha}{2+e_2}\right]-a^2+\frac{Hab}{2+e_2}=0$$

where the inequality is expressed in terms of the tangents of longitudinal angles. For convenience this can be written

$$Ax^2+Bxy+Cy^2+Ey+F=0.$$

[50] Reference 11, p. 620. See also Ames, Gliddon and Ogle, *Size and Shape of Ocular Images, I*, Archiv. of Ophth., *7*, 588; 1932.

To find the degree of rotation of the horopter it is only necessary to determine the tangent to the curve at the fixation point $(0, b)$. (Fig. 22.) Thus

$$dy/dx]_{0,b} = -Bb/(2Cb + E).$$

Let R be the angle of rotation of the longitudinal horopter from the frontal plane for a percent size change of the longitudinal angles in the right eye of $100e_2$. Then substituting the equivalents for B, C and E, and reducing one obtains

$$\tan R = dy/dx]_{0,b} = [e_2/(2 + e_2)](b/a) \qquad (49)$$

where b is the fixation distance and $2a$ is the nodal point base line. It is apparent from the equation that theoretically this rotation of the longitudinal horopter and therefore the field of binocular single vision about the fixation point will vary directly with the value of b, i.e., the fixation distance. With the use of Eq. (49), Table 9 has been computed, which

TABLE 9

Percent difference in size of ocular images $100e_2$	Fixation distance 0.164 D b=6.1 m	1.33 D 75.6 cm	2.50 D 40.4 cm	4.94 D 20.0 cm
0.5%	25°09	3°32	1°77	0°87
1.0%	43°05	6°61	3°54	1°75
1.5%	54°42	9°83	5°29	2°62
2.0%	61°72	12°98	7°02	3°48
3.0%	70°18	18°99	10°42	5°19
6.0%	79°64	34°15	19°92	10°15

a=32.5 mm.

shows the degree of rotation of the visual field that should be produced theoretically by various percentages of increase of one of the ocular images for various fixation distances. That these values do represent the actual rotation of the empirical horopter resulting from the increase of the ocular image of one of the eyes by a lens, has been shown experimentally.[50] Because of symmetry, the degree of rotation of the longitudinal horopter produced by a change in the ocular image of the left eye will be equal to the above values, but reversed in direction. It should be noted that theoretically the rotation of the horopter about the fixation point is independent of the shape of the horopter and independent of the particular choice of the perspectival center, for it depends only on ratio b/a which is defined by the convergence of the eyes.

B. DISTORTION OF THE HOROPTER

The deviation of the trace of the symmetrical longitudinal horopter from the Vieth-Müller circle can be interpreted as being due to an asymmetrical difference in the longitudinal angles of corresponding points in the two eyes. Since such an asymmetry or distortion is produced by ordinary prisms it is important to know its nature and magnitude. This distortion found in prisms is usually measured in terms of the percent increase of the longitudinal angle for any given angular oblique ray which would pass through the nodal point of the eye if such a lens were

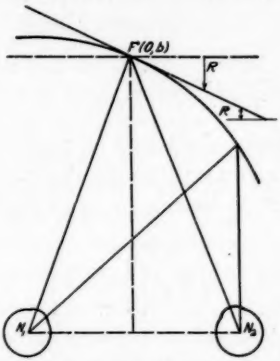

FIG. 22. *A diagram for finding the magnitude of the apparent rotation of the visual field, for a given change in ocular image size between the two eyes.*

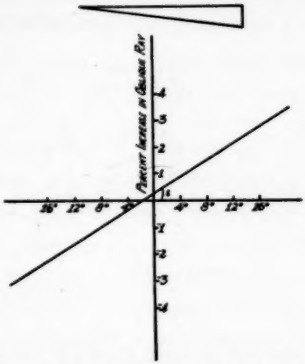

FIG. 23. *Schematic graph of the distortion curve of a flat prism.*

placed before it. Fig. 23 shows graphically the typical distortion curve of an ordinary flat prism.[51] Thus the percentage increase in angular size across the prism may be denoted by the slope of the line h, considered positive in direction of the base of the prism. The overall magnification of the angles e is determined by the intercept on the ordinate axis. The effect of such a prism placed before the right eye, with apex to the left (base out), on the magnification at any angle will be given by

$$n_2 = 1 + h_2 w_2 + e_2.$$

Substituting this in the fundamental longitudinal horopter equation one has

$$1/w_1 - (1 + h_2 w_2 + e_2)/w_2 = H. \qquad (50)$$

[51] Reference 11, p. 622 ff. See also Ames, Gliddon and Ogle, *Lenses for Changing the Size and Shape of Dioptric Images*, The Annals of the Dist. Serv. Found. of Optom., *1* (1) p. 61; 1932.

Reduction to the analytical form (Eqs. 11 and 16) gives

$$P = (w_2 - w_1)/w_1 = (H + h_2)w_2 + e_2. \tag{51}$$

This equation is descriptive of a horopter trace with an increased value of the Hering-Hillebrand horopter deviation, i.e., with a decreased concavity toward the observer.

The effect on the horopter trace of a prism placed before the left eye apex to the left (base-in), is given by

$$(1 + h_1w_1 + e_1)/w_1 - 1/w_2 = H \tag{52}$$

which reduces to the analytical form,

$$P = \frac{w_2 - w_1}{w_1} = (H - h_1)\frac{w_2}{1 + e_1} - \frac{e_1}{1 + e_1} \tag{53}$$

which is descriptive of a horopter trace with a decreased Hering-Hillebrand horopter deviation, i.e., with greater concavity to the observer.

The effect on the horopter trace of prisms base-in, in both eyes is given by

$$P = \frac{w_2 - w_1}{w_1} = (H - h_1 - h_2)\frac{w_2}{1 + e_1} - e_2 + e_1\left[\frac{1 + e_2}{1 + e_1}\right] \tag{54}$$

or base-out in both eyes by

$$P = \frac{w_2 - w_1}{w_1} = (H + h_1 + h_2)\frac{w_2}{1 + e_1} + e_2 - e_1\left[\frac{1 + e_2}{1 + e_1}\right]. \tag{55}$$

If prisms with equal distortion and overall magnifications are placed before the eyes with both bases the same direction, that is, if $h_1 = -h_2$, the Hering-Hillebrand deviation remains unaffected.

The closeness with which such analysis represents the nature and magnitude of the distortion effect that is actually produced on the empirical horopter by prisms, has been shown in another paper.[51] It is clear from the above development that if the equation of the distortion curve of any lens can be determined, and that lens be used before the eye it is possible to show the effect it should have upon the shape of the horopter. Thus, suppose the difference quotient $P = (w_2 - w_1)/w_1$ of a lens at any oblique ray be given by

$$P = f(w_2) + e_2 \tag{56}$$

where again $100e_2$ will represent the overall percent magnification. If such a lens is placed before the right eye, for example, one can write

$$1/w_1 - (1 + f(w_2) + e_2)/w_2 = H \tag{57}$$

which reduces to the analytical form within the precision of measurements,[52]

$$P = (w_2 - w_1)/w_1 = Hw_2 + f(w_2) + e_2. \tag{58}$$

To some extent the converse holds, i.e., the residual distortion between the two eyes as indicated by an empirically determined horopter can be found.

IX. Application of Analysis to the Longitudinal Magnitude of the Fusional Areas or Panum's Circles of Sensation

For a given convergence of the eyes, there exists a three-dimensional region in space across the visual field within which point objects are seen binocularly single. Corresponding to this region, effective areas must exist on the retinas within which similar images will be fused. In general, the region includes the point of fixation, but more importantly the horopter. Hence, the images of points that lie within the region, but not actually on the horopter, will be disparate images relative to the nearest pair of corresponding points. The farther a given point lies from the horopter, the greater will be the angular disparity of the images, and at the boundaries of the region of binocular single vision the magnitude of the disparity will have reached the limit of fusional power. Beyond this boundary, points will appear double, though in general one or both may be suppressed.[53] Thus in general, surrounding each of a pair of corresponding points there exists an effective area of sensation within which similar images will be fused and will appear binocularly as one. Fischer and Tschermak[54] have shown that the horopter apparatus is suitable for determining the region of binocular single vision. The two limiting positions where doubling occurs can be found[55] by the rapid movement of the vertical threads in the various lanes. It remains now to investigate to what extent the longitudinal magnitude of these fusional areas can be determined when points on the boundaries

[52] Perhaps it should have been stated earlier, that when the image in one eye is altered by a given distorting or magnifying lens, besides the effect of this change a new distortion may creep in due to the unbalancing of the aberrations in the two eyes. This can be shown to have a very secondary effect upon the horopter in general for changes ordinarily produced. In certain cases, however, the effect may be detected in the horopter data and as such prove a means of measurement.

[53] Tschermak and Hoefer, Pflüger's Arch., *98*, pp. 299–321; 1903.

[54] F. P. Fischer, Pflüger's Arch., *204*, pp. 234–246; 1924.

[55] Reference 11, p. 591.

of the region of binocular single vision are treated according to the analytical devices of the previous sections.

For purposes of diagrammatic representation Fig. 24 will be used. Let F be the point of fixation, which, if for the present no fixation disparity is assumed, will lie on the horopter. Let P_0 be a point on the horopter, determined by corresponding points having longitudinal angles α_1 and α_2 of the left and right eyes, respectively. Now, areas of sensation that include each of the corresponding points will have objective angular magnitudes. A study of the figure shows schematically how the outer and near limits of the region of single binocular vision corresponding to effective areas on the retinas, are determined by the

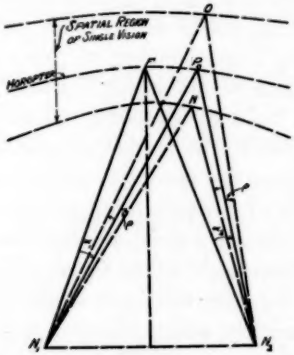

FIG. 24. *Diagram used for the study of Panum's fusional areas.*

intersection of the visual lines proceeding from the longitudinal edges of these areas. For purposes of development consider the outer or homonymous limit 0, of the region, for the longitudinal angle α_2 of the right eye. This point will be determined by the small angles ρ_1 and ρ_2 of the homonymous halves of the fusional areas of the left and right eyes, respectively, measured positively clockwise. Imposing this condition upon the fundamental horopter Eq. (5), assuming no inequality of ocular images or presence of fixation disparity one has

$$1/(w_1 + r_1) - 1/(w_2 - r_2) = H \tag{59}$$

where $r_1 = \tan \rho_1$ and $r_2 = \tan \rho_2$. Reducing this equation to the form used in the analytical graph, one has

$$Hw_2^2 - w_2P(1 - Hr_1) + w_2H(r_1 - r_2) + [(r_1 + r_2) - Hr_1r_2] (1 + P) = 0 \tag{60}$$

where $P=(w_2-w_1)/w_1$. The corresponding equation for the inner or heteronymous limits, N, is obtained by changing the signs of r_1 and r_2 in 60. Thus

$$Hw_2^2 - w_2P'(1 + Hr_1') - w_2H(r_1' - r_2') - [(r_1' + r_2') + Hr_1'r_2'](1 + P') = 0. \quad (61)$$

Eqs. (60) and (61) represent two hyperbolas which are nearly conjugate to each other. All four branches will appear on the analytical graph representing the whole region of binocular single vision. An illustration from actual data is given in Table 10 and shown in the spatial and analytical graphs, Figs. 25 and 26.[56]

TABLE 10. *Data of K.N.O. for the spatial region of binocular single vision determined on the horopter apparatus at b=404 mm.*

	Outer limits										
	Left field						Right field				
LANE	12°	8°	4°	2°	1°	0	1°	2°	4°	8°	12°
Mean position outer limits mm	+7.5	+5.5	+2.4	+2.7	+2.5		+3.3	+3.1	+3.5	+3.7	+3.0
Mean dev. mm.	±3.9	±2.5	±1.8	±0.9	±0.4		±0.8	±1.2	±1.7	±3.2	±5.1
Percent value of mean position from iso-mag. curves	−4.9	−3.9	−2.5	−3.6	−5.6		+8.0	+4.1	+3.2	+3.5	+4.3
Percent mean dev.	±0.7	±0.7	±1.1	±1.1	±0.9		±1.8	±1.4	±1.0	±0.9	±1.0
	Near limits										
Mean position near limits mm	−10.3	−6.8	−3.4	−2.2	−2.0		−2.1	−2.6	−4.6	−9.2	−15.3
Mean dev. mm	±1.2	±1.1	±1.0	±0.5	±0.6		±0.3	±0.4	±1.1	±1.7	±2.9
Percent value of mean position from iso-mag. curves	−1.6	−0.4	+0.7	+2.0	+4.5		−4.4	−2.4	−1.4	−0.3	+0.7
Percent mean dev.	±0.2	±0.3	±0.6	±0.6	±1.4		±0.7	±0.5	±0.7	±0.5	±0.6

Throughout this paper it has been emphasized that the most fruitful method of representing points in the visual field is not in terms of x, y coordinates, but in terms of a longitudinal angle of one of the eyes, w_2, and the difference quotient $P=(w_2-w_1)/w_1$ of the tangents of the longitudinal angles to the point measured from the fixation lines. This transformation is possible through the iso-magnification curves. Now, points on the boundaries of the region of binocular single vision should also be so represented as shown in Fig. 26. Eqs. (60) and (61), representing

[56] *Size and Shape of Ocular Images, III.* Arch. of Ophth. 7, p. 12 ff., 1932.

the curves on this graph, show the relation which must exist between P and w_2 for a given value of H and the values of either the homonymous or heteronymous halves of the fusional areas. It is clear from inspection that if P and w_2 are known for a point on the boundary, the individual angles r_1 and r_2 cannot be found. Now the order of magnitude of r_1 and r_2 is near 0.003, hence Eqs. (60) and (61) can be simplified within the error of precision of the measurements, to

$$Hw_2^2 - w_2P + (r_1 + r_2)(1 + P) = 0 \tag{62}$$

$$Hw_2^2 - w_2P' - (r_1' + r_2')(1 + P') = 0 \tag{63}$$

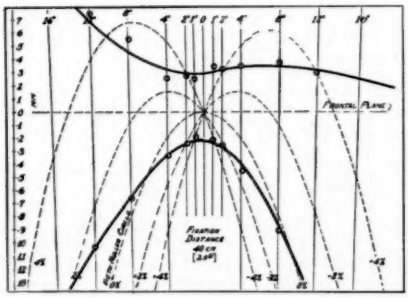

FIG. 25. *Representation of the region in space of single binocular vision. Data of K.N.O.*

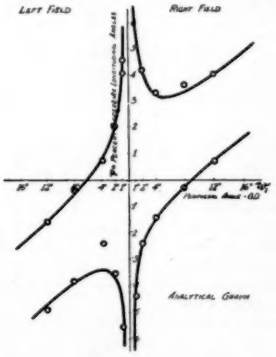

FIG. 26. *Analytical representation of the region of binocular single vision. Data of K.N.O.*

where (62) refers to the outer boundary and (63) to the inner boundary. Thus only the sum of the homonymous or heteronymous halves of the fusional areas of both eyes can be obtained. However, the mean area can be found for a given peripheral angle w_2 if P and P' are known for the outer and inner boundaries. Let A_1 and A_2 be the angular sizes of the fusional areas of the left and right eyes, respectively, then the mean value A will be, from (62) and (63),

$$A = \tfrac{1}{2}(A_1 + A_2) = (r_1 + r_1') + (r_2 + r_2') = (r_1 + r_2) + (r_1' + r_2').$$

Hence,

$$A = \tfrac{1}{2}\left[\frac{w_2P - Hw_2^2}{1 + P} - \frac{w_2P' - Hw_2^2}{1 + P'}\right]. \tag{64}$$

Within the precision of measurements this can be written

$$A = (w_2/2)(P - P'). \tag{65}$$

In general, however, a fixation disparity will exist and will slightly modify the position of the region in space and the shape of the analytical curves. This is easily taken into account, however. Referring to the preceding section, if a fixation disparity does exist, the fundamental equation for the fusional areas becomes

$$1/[(w_1 - s) + r_1] - 1/[(w_2 + s) - r_2] = H \tag{66}$$

for the outer boundary, and for eso-fixation disparity (s taken positive). This can be written

$$1/[w_1 + (r_1 - s)] - 1/[w_2 - (r_2 - s)] = H$$

and immediately the analytical equivalent can be written, *viz.*,

$$Hw_2^2 - w_2P(1 - H(r_1 - s)) + w_2H(r_1 - r_2) + [(r_1 + r_2 - 2s) - H(r_1 - s)(r_2 - s)][1 + P] = 0. \tag{67}$$

Simplified this can be written

$$Hw_2^2 - w_2P + (r_1 + r_2 - 2s)(1 + P) = 0. \tag{68}$$

Likewise for the near boundary

$$Hw_2^2 - w_2P' - (r_1' + r_2' + 2s)(1 + P') = 0. \tag{69}$$

The average value of A, when P and P' are known for a given angle α_2, will be the same as Eq. (64), for while the fixation disparity angle in the case of eso-fixation disparity decreases the apparent magnitude of the homonymous halves of the fusional areas, it increases the heteronymous halves so that the average magnitude remains unchanged within greater precision than the measurements. Furthermore, within the precision of measurements, any inequality in the size of the ocular images will not enter the problem when the data are in the analytical form.

By using Eq. (64), the mean angular longitudinal values of the fusional areas[57] for the various peripheral angles from the data of Table 10 are computed[58] and are given in Table 11, and are shown graphically in Fig. 27.[56]

[57] Reference 12, p. 894 ff. The values obtained here are probably between Tschermak's relative and absolute values, probably much nearer the latter.

[58] These data were obtained with apparatus in which the lanes converged to the median nodal point and not to the mean nodal point of the right eye as would be demanded by the theory presented. The relation between w_2 and the lane angle ϕ for points in the vicinity of the frontal plane for a fixation distance of 400 mm can be shown to be $w_2 = \tan\phi/(1.007 = 0.08 \tan\phi)$. Thus a small error occurs in the above computation which is greater for large values of ϕ but which is below the precision of measurements and hence will be neglected.

TABLE 11. *Angular longitudinal magnitudes of the fusional areas computed from Table 10 from Eq. (20) for K.N.O. at 2.5 D.*

	Left field						Right field				
Lane	12°	8°	4°	2°	1°	0	1°	2°	4°	8°	12°
Minutes of arc	12.5	8.6	3.8	3.4	3.0		3.6	3.9	5.5	9.1	13.1

X. THE CIRCLE APPROXIMATION OF THE LONGITUDINAL HOROPTER

In the preceding sections it has been shown that the longitudinal horopter may follow a general law expressed in Eq. (5), which determines a one or two parameter family of conic sections illustrated for the one parameter case in Fig. 4. This concept followed from the assumption that there may exist for an individual a distance where the longitudinal horopter would lie in the fixation frontal plane, i.e., the existence of the abathic surface. Furthermore, it was shown that the symmetrical

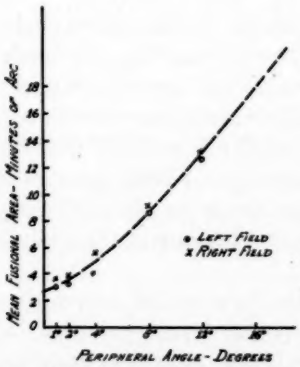

FIG. 27. *Graph illustrating change in horizontal magnitude of Panum's fusional areas with peripheral angle.*

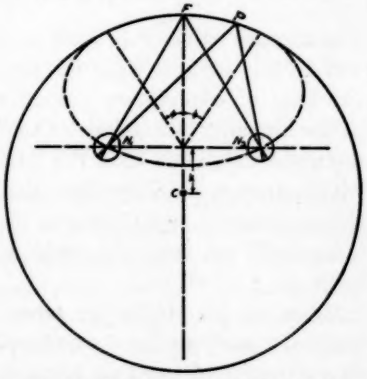

FIG. 28. *The circle approximation to the longitudinal horopter.*

longitudinal horopter could then be specified by a single parameter H which expresses quantitatively the Hering-Hillebrand deviation. Experimental data indicate that in general the empirical longitudinal horopter falls into the class of curves corresponding to ellipses in the above theory and this is reasonably substantiated in that the analytical

transformation of the data follows the linear Eq. (11). However, circles can be drawn which approximate these ellipses save for large peripheral angles. But within 16°, the precision of measurements of experimental data and the increased separation of contiguous iso-magnification curves for the larger peripheral angles, increase the uncertainties in trying to fit the data to one or the other type of curves. It is of interest, however, to study the circles which may be used as approximations for the system of ellipses in finding the positions of their centers for different values of the Hering-Hillebrand deviation constant.[59] Just what constitutes an approximation of the two curves is a question. Keeping in mind, however, the experimental findings of the longitudinal horopter and the region in which it is found, one can find only the approximate center of the circle in any case. Since the departure of the ellipse from the circle within the visual field where data are available is relatively small, that circle will be considered which includes a point on the ellipse at a given peripheral angle. This treatment is quite inadequate for the complete range of values of H, but it is sufficient within the range indicated by experiment. Only the symmetrical horopter will be examined.

It has been shown that the spatial curve representing the symmetrical longitudinal horopter specified by a given H, could be expressed by

$$x^2\left[1 - H\frac{b}{2a}\right] + y^2\left[1 + H\frac{a}{2b}\right] - y\left[\frac{b^2 - a^2}{b} + Ha\right] - \left[a^2 - H\frac{ab}{2}\right] = 0 \qquad (6)$$

where $2a$ is the length of the mean nodal point base line and b is the fixation distance from the latter. Within the range of experimental values of H, this equation expresses an ellipse which passes through the point of fixation and the two mean nodal points of the eyes. Now the general equation of a circle which will pass through the point of fixation and whose center is on the ordinate axis a distance k from the origin is

$$x^2 + (y - k)^2 = (b - k)^2. \qquad (70)$$

If, now, a point is taken common to both curves for a given peripheral angle ϕ, see Fig. 28, one has the additional relation

$$x = y \tan \phi. \qquad (71)$$

[59] Fischer and Tschermak use this circle representation in describing some of their results. Reference 54, p. 203.

From these three equations one can find k in terms of H and the angle ϕ. For the values of H varying between zero and $H=2a/b$ for the frontal plane, Fig. 29 shows the graphic relation between k and H, computed for a fixation distance of 404 mm, a nodal point base line of 65 mm and $\phi=10°$. Referring to the data of K.N.O., Fig. 12, one finds that for $H=0.13$, k is near -350 mm, which indicates that the center of the circle which approximates the data is nearly 35 cm behind the mean nodal point base line, behind the observer. Moreover, computation based upon the experimental values of H shows that the center recedes very rapidly for increased fixation distances. It is clear that the representation of horopter data following the fundamental horopter equation

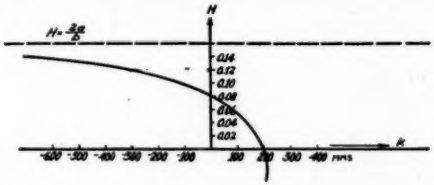

FIG. 29. *Graph showing position of the center of the circle approximation to the longitudinal horopter for a given Hering-Hillebrand deviation value.*

as developed in this paper is far superior to and more fruitful than any circle type representation.

XI. THE PRECISION OF MEASUREMENTS

Table 12 records the mean deviations of a large number of settings of the wires in horopter determinations made by several criteria at various fixation distances, expressed in terms of the difference quotient $P=(w_2-w_1)/w_1$ in percent, for the different lanes of the apparatus.[60]

TABLE 12. *Mean deviations for peripheral angle in percent P.*

Fixation distance diopters	Data of K.N.O. Apparent frontal plane						
	1°	2°	4°	8°	12°	16°	Readings
0.164 (6.1 m)	—	0.07%	0.03%	0.04%	0.03%	—	18
1.33 (75.6 cm)	0.19%	0.14%	0.10%	0.12%	0.12%	0.12%	70
2.50 (40.4 cm)	0.33%	0.21%	0.15%	0.16%	0.16%	0.21%	240
4.94 (20.0 cm)	—	0.44%	0.43%	0.31%	0.39%	0.56%	82

[60] Reference 56, p 8. ff.

Fixation distance diopters	Data of F.D.C. Apparent frontal plane						
	1°	2°	4°	8°	12°	16°	Readings
0.164 (6.1 m)	0.10%	0.08%	0.06%	0.07%	0.07%	—	60
1.33 (75.6 cm)	0.39%	0.31%	0.22%	0.21%	0.25%	0.33%	10
2.50 (40.4 cm)	0.57%	0.54%	0.50%	0.59%	0.72%	—	104
4.94 (20.0 cm)	—	1.60%	0.97%	0.76%	1.04%	1.02%	12

Fixation distance diopters	Data of K.N.O. Grid-nonius horopter						
	1°	2°	4°	8°	12°	16°	Readings
1.33 (75.6 cm)	0.57%	0.49%	0.34%	0.31%	0.19%	—	44
2.50 (40.4 cm)	0.89%	0.56%	0.47%	0.48%	0.48%	—	450
4.94 (20.0 cm)	—	2.00%	2.04%	1.26%	1.32%	1.17%	72

The greater increase in the errors at 4.94 diopters is due primarily to the fact that the magnitude of the personal errors approaches that of the errors of the apparatus.

These are only representative results. Less experienced observers undoubtedly would have somewhat larger mean deviations. With these experimental deviations as a basis for reference, the limit of error can be found which is permissible in the adjustment of the head.

A. ERROR IN FIXATION DISTANCES

It is clear that for a given point in the visual field, x, y, the percent difference quotient of longitudinal angles to it can be found from solving Eq. (21) for $e_2=P$, *viz.*,

$$P = \frac{-2[x^2 + y^2 - y(b^2 - a^2)/b - a^2]}{[x^2 + y^2 - y(b^2 - a^2)/b - xy(b^2 + a^2)/ab - a^2]}. \qquad (72)$$

Considering a point in the fixation frontal plane as representative, one substitutes $y=b$, then

$$P = -2x/(x - bR) \qquad (73)$$

where $R=(a^2+b^2)/ab$. Hence the change in P for a small change in the fixation distance will be

$$dP/db = -4(b/a)[x/(x - bR)^2]. \qquad (74)$$

For the smaller fixation distance there will be a greater error in the

transformation of data, due to an inaccuracy of adjusting the eyes of the observer for the correct fixation distance. Table 13 has been computed to show that error for a fixation distance of 404 mm. The quantity

TABLE 13. *Values of dP/db for a=32.5 in percent P.*

Fixation distance	Lane angle ϕ 1°	2°	4°	8°	12°	16°
756.8 mm	−0.0004	−0.0008	−0.0016	−0.0031	−0.0047	−0.0063
404.3 mm	−0.0014	−0.0028	−0.0056	−0.0113	−0.0173	−0.0236
199.8 mm	−0.0054	−0.0107	−0.0211	−0.0416	−0.0615	−0.0811

$[dP/db]$ will be expressed in the percent difference quotient error in longitudinal angles to a given point per millimeter error in adjusting the eyes of an observer for the correct fixation distance for which the iso-magnification curves have been computed in the transformation of the data. It is clear at once that an error of several millimeters would be far below the mean deviation of experimental data.

B. ERROR IN INTERPUPILLARY DISTANCE OR MORE SPECIFICALLY THE NODAL POINT BASE LINE

In general the iso-magnification curves (and transformation graphs) are computed for a given fixation distance and a given nodal point base line. It is desirable to know, then, what error will occur in the transformed values for a given point for small variations of the nodal point base line (hence interpupillary distance). Differentiating then Eq. (72) relative to a for representative points on the fixation frontal plane one has

$$dP/da = 2xbS/a^2(x - br)^2 \tag{75}$$

where $S=(b^2-a^2)/b$ and $R=(a^2+b^2)/ab$. Table 14 has been computed to show dP/da, the error in the percent difference quotient for longitudinal angles to a given point on the fixation frontal plane introduced

TABLE 14. *Values of dP/da for a=32.5 in percent P.*

Fixation distance	Lane angle ϕ 1°	2°	4°	8°	12°	16°
756.8 mm	0.0046	0.0091	0.0183	0.0365	0.0549	0.0735
404.3 mm	0.0084	0.0169	0.0336	0.0669	0.0997	0.1330
199.8 mm	0.0161	0.0319	0.0633	0.1244	0.1840	0.2427

per millimeter change in a (per two millimeter change in nodal point base line) for three different fixation distances.

Eqs. (74) and (75) show that the transformation value of a given point will be too large for a small increase in the fixation distance and will be too small for a small increase in the nodal point base line. Inasmuch as the latter for a given individual cannot be changed, it is clear that the effect of any small difference in nodal point base line from that for which the iso-magnification curves were computed could be counterbalanced by a change in the fixation distance. Then

$$(4b/a)[x/(x - bR)^2]db = (2bS/a^2)[x/(x - bR)^2]$$

whence

$$db = (S/2a)da = [(b^2 - a^2)/2ab]da. \tag{76}$$

Thus, the effect of an increase in the nodal point base line of 2 mm, could be compensated by an increase in the fixation distance for 20 cm of 3.0 mm; for 40 cm of 6.2 mm; and for 75.6 cm of 11.6 mm. In general, however, small variations in a and b from those used in the iso-magnification curves are left uncorrected since the error introduced is below the precision of the experimental data.

C. ERROR DUE TO SLIGHT ROTATION OF THE HEAD

Asymmetrical convergence results from a slight rotation of the head in the horopter apparatus. In order to find the error introduced in the data as interpreted from the iso-magnification curves, the expression for the difference quotient of longitudinal angles to a given point must be found. Referring to Fig. 30, suppose the head is rotated to the left by an angular amount ψ, then one can write for the longitudinal angles to a given point

$$w_1 = \frac{(b + C)(x + B) - B(y + C)}{(x + B)B + (y + C)(b + C)}$$

and

$$w_2 = \frac{B(y - C) + (b - C)(x - B)}{(y - C)(b - C) - B(x - B)}$$

where $B = a \cos \psi$ and $C = a \sin \psi$. By sustituting in the expression

$$n_2 = 1 + P = w_2/w_1$$

and as before, considering representative points on the fixation frontal plane, $(y = b)$, one has.

$$n_2 = 1 + P = \frac{[x(b-C)][B(x+B)+(b+C)^2]}{[(b-C)^2 - B(x-B)][(b+C)x]}.$$

The error in P caused by a slight rotation of the head can be found by

$$\left.\frac{dP}{d\psi}\right]_{\psi=0} = \left.\frac{dn_2}{d\psi}\right]_{\psi=0} = \left[\frac{2a}{b}\right]\left[\frac{b^2 - ax - a^2}{(b^2 + a^2 - ax)^2}\right][a^2 + b^2]. \qquad (77)$$

Inspection of this expression shows that the peripheral angle enters only secondarily and that within the precision of measurements the error introduced in the transformation of data from the original iso-magnification curves when the head has rotated about the midpoint of the nodal point base line is a constant throughout the visual field. This is equivalent to a simple percent overall magnification. Table 15 has been

TABLE 15

Fixation distance	20 cm	40 cm	75.6 cm	606.0 cm
Error in P per degree rotation of head (percent)	0.55	0.28	0.15	0.019

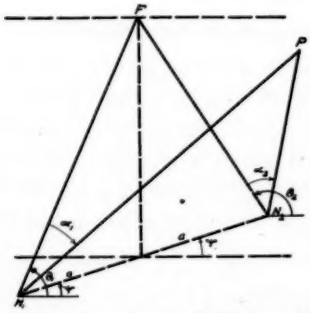

FIG. 30. *Diagram used to find error introduced in horopter data due to a small rotation of the observer's head.*

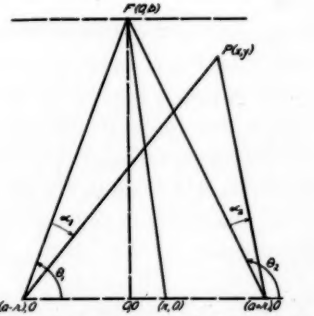

FIG. 31. *Diagram used to find error introduced in horopter data due to a lateral displacement of the observer's head.*

computed from Eq. (77) to show the magnitude of the error in P (i.e., $(w_2 - w_1)/w_1$) for a rotation of the head one degree for various fixation distances and for an average peripheral angle of 8°. Thus, if the head be incorrectly adjusted in the horopter apparatus so that it is rotated one degree counterclockwise (looking right), the transformed data will show an erroneous enlargement of the ocular image in the right eye

by the magnitudes shown in Table 15. Extensive computation on asymmetrical convergence shows that this error increases proportionally to the angle of rotation of the head about the midpoint of the nodal point base line. Hence experimental studies on the horopter with asymmetrical convergence can be made by using the transformation curves for symmetrical convergence and by making the proper correction. The most important single adjustment of the head in the apparatus is then, that for symmetrical convergence. However, if the variations in the Hering-Hillebrand deviation that are desired from a given set of data, the overall effect of slight rotations can be neglected.

D. ERROR DUE TO LATERAL DISPLACEMENT OF THE HEAD

If the observer's head in the apparatus is displaced to one side of the median plane, asymmetrical convergence again results. In order to determine the magnitude of the error for a point in the visual field, it is only necessary to set up equations specifying the longitudinal angles to that point with the displaced head. In Fig. 31 let the head be displaced to the right r mm. Then

$$w_1 = [b(x + a - r) - (a - r)y]/[(a + r)(x - a - r) + by]$$

and

$$w_2 = [(a + r)y + b(x - a - r)]/[by - (a + r)(x - a - r)].$$

For this discussion consider only representative points in the fixation frontal plane, thus putting $y = b$, and substituting in

$$n_2 = 1 + P = w_2/w_1.$$

one has

$$n_2 = 1 + P = [(a - r)(x + a - r) + b^2]/[b^2 - (a + r)(x - a - r)]$$

The change in P for a point in the fixation frontal plane due to a small displacement of the head to the right can be found from

$$\left.\frac{dP}{dr}\right]_{r=0} = \left.\frac{dn_2}{dr}\right]_{r=0} = -\frac{2a[2(a^2 + b^2) - x^2]}{[a^2 + b^2 - ax]^2}. \qquad (78)$$

By the use of this equation, the error introduced per millimeter displacement of the head has been computed for average points at four

fixation distances. (Table 16.) By comparing these representative deviations with the empirical deviations of Table 13, it is clear that the rotational adjustment of the head is the most important of the adjustments. This is closely followed in importance by that for lateral displacement of the head.

TABLE 16. *Error introduced in value of P for an average point in fixation frontal plane when head is displaced 1 mm to right.*

Fixation distance	20 cm	40 cm	75 cm	606 cm
Error in percent difference in *P*	0.33	0.08	0.02	0.0003

ACCOMMODATION, PUPILLARY WIDTH AND STIMULUS DISTANCE*

By Ellis Freeman

[University of Louisville, Louisville, Kentucky.

Received August 30, 1932]

In earlier papers[1,2,3,4] an anomaly of visual acuity has been studied which consists of a markedly greater acuity for a large distant constellation than for a small and correspondingly near constellation. Such an anomaly is obviously a violation of the principles of geometrical projection upon which Snellen and other acuity tests are based. Assuming the principles of geometrical projection to be valid, one would naturally seek an explanation for the stubborn persistence of this anomaly in some sort of dioptrical inequalities between the adjustment of the eye for the large and for the small constellations. These inequalities would consist of a wide pupil and thin lens for the large constellation and a narrow pupil and thick lens for the small. It has been *indirectly* shown,[3] and with relation to pupillary width it has been demonstrated directly,[4] that dioptrical mechanisms may not be held accountable.

In order to investigate the matter *directly*, thoroughly, and extensively, the following experimental investigation has been made to determine the influence of accommodation and pupillary width on this anomaly. The apparatus and conditions of observation were like those already described,[4] with the addition of appropriate lenses to control accommodation, and in one series an artificial pupil of 1 mm diameter for the maintenance of constant pupillary width for both constellations. All observations were monocular after 30 minutes of dark-adaptation. Subject 2 was one of the two used for the original investigation a year before,[4] and Subject 3 was new.

The subject was presented with a homogeneously illuminated field

* This work, like the original, was made possible by a grant from the Howe Fund of the Harvard Medical School, and by the interest and generous assistance of Dr. Frederick H. Verhoeff, Professor of Ophthalmic Research. It was carried out in the Howe Laboratory of Ophthalmology of the Massachusetts Eye and Ear Infirmary.

[1] Ellis Freeman, *Untersuchungen über das indirekte Sehen*, Psychologische Forschung, *14*, 3/4, pp. 332–365; 1931.

[2] Ellis Freeman, *Anomalies of Peripheral Visual Acuity*, J. of Exper. Psych., *12*, pp. 324–340; 1929.

[3] Ellis Freeman, *Anomalies of Visual Acuity in Relation to Intensity of Illumination*, Amer. J. Psych., *42*, pp. 287–294; 1930.

[4] Ellis Freeman, *Anomalies of Visual Acuity in Relation to Stimulus-Distance*, J.O.S.A., *22*, pp. 285–292; 1932.

(50×50 cm at a distance of 300 cm, and 5×5 cm at a distance of 30 cm) traversed by two vertical metal bars (50×5 cm for the large constellation, and 5×0.5 cm for the small constellation). From where he sat at the ocular of the apparatus he made an adjustment of the bars from closed to barely separated, that is he resolved them minimally to give the so-called *minimum separable*. In each table under the caption of 'slit' is given the average of four such resolutions. The *MV* for each slit value in the table has not been printed in order to avoid unwieldiness of format; it is, however, of the same order as the values published originally.[4] Thus, what the subject dealt with in making his minimum separable adjustments was a weakly illuminated field against which stood the *totally unilluminated* bars. It is obvious that for both constellations the retinal images were identical in size, intensity, and position. As a further check, in addition to photometrizing from the ocular of each apparatus, photographic time exposures were made from the oculars of both constellations, with the slit open at 4 cm for the large and 0.4 cm for the small. To keep the same 'draw' of the camera for both constellations, so that the plate would receive the same density of light for each, a minus 3D lens was placed at the ocular of the large constellation, and to make a correction for the loss of light entailed by the interposition of this lens a plano lens was placed at the ocular of the small constellation. The resulting photographic plates show that the two images delivered to the eye were identical in size and intensity. Consequently, as far as the physical conditions at the oculars were concerned, the two constellations were treated precisely alike, and the anomaly must be a function of the eye itself.

It might be argued that with the small constellation, since the eye was accommodated to 30 cm, the thicker lens caused a relative loss of acuity because a thicker lens is perhaps a less efficient optical instrument and therefore gives a less well-defined image, or simply because it interposes relatively more lenticular medium it absorbs more light in transmission and thus reduces acuity. To meet this situation a plus 3.50D lens was placed at the eyepiece of the small constellation, and a plus 0.25D lens at the eyepiece of the large constellation. These two lenses rendered the crystalline totally and equally *unaccommodated* for both constellations. The conditions might, therefore, be regarded as identical for the eye in both constellations, except that the stronger lens, being thicker, interposed more absorbing material with the small constellation, and thus might have caused a loss of acuity. This source of error is of relatively little consequence, because the greatest loss of light

in lenses is due to reflection and not to absorption. Nevertheless, a means was provided, as described below, to compensate for this by the employment of a minus thick lens with the large constellation and a minus thin lens with the small, thus balancing the disadvantages.

For the present it is significant to note that with plus lenses ruling out all differences in accommodation of the crystalline, the anomaly appears just as before.[4] Table 1, gives the data showing this both in

TABLE 1. *Minimum separable, under dark-adaptation.*

	Subject 2		Subject 3		
Log I	Slit	Acuity (1/slit)	Slit	Acuity (1/slit)	Average acuity
	Large constellation (with plus 0.25D lens at eyepiece)				
−3.02855	1.3 mm	0.77	1.6	0.62	0.69
−3.32098	1.9	0.53	1.9	0.52	0.52
−3.61341	3.5	0.29	2.1	0.48	0.38
−3.90584	4.1	0.24	3.5	0.29	0.26
−4.19827	5.5	0.18	4.4	0.23	0.20
−4.49070	5.8	0.17	5.8	0.17	0.17
		(1/slit×10)		(1/slit×10)	
	Small constellation (with plus 3.50D lens at eyepiece)				
Same as above	0.4	0.25	0.5	0.20	0.23
	0.6	0.17	0.6	0.16	0.17
	0.9	0.11	0.8	0.13	0.12
	1.0	0.10	0.9	0.11	0.11
	1.4	0.07	1.0	0.10	0.09
	1.7	0.06	1.1	0.09	0.08

terms of slit-width and of acuity. Fig. 1 gives the curves for the average acuity of the two subjects for each constellation and also the acuity values for each subject individually. A fact of importance is that there is no overlapping between any of the values of the large and any of the small constellation. This shows that the two curves represent definitely independent acuity functions.

In order to provide a means of balancing the disadvantages of a thick lens, the eyepiece of the large constellation was provided with a minus 3.50D lens, and the eyepiece of the small with a minus 0.25D lens. Thus conditions as to the thickness of interposed glass were reversed, and now the large constellation was handicapped. Whereas for Table 1 both constellations were viewed with an equally unaccommodated crystal-

line; here, for the results in Table 2 and Fig. 2, both constellations were viewed with an equally *accommotated* crystalline. Again the anomaly appeared in pronounced form, with a persistently higher acuity for the

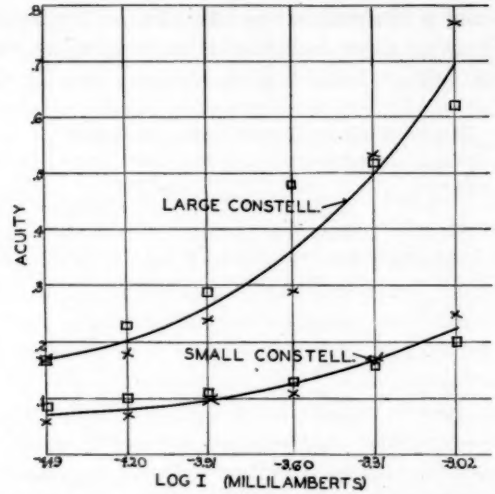

FIG. 1. *Showing disparity in acuity between large and small constellations. Based on Table 1. Lines correspond to "average acuity" of both subjects. Crosses represent values for Subject 2, and squares for Subject 3. As there is no overlapping between the two constellations, the curves represent definitely independent acuity functions. Crystalline maintained at zero accommodation for both constellations by the use of appropriate plus lenses.*

TABLE 2. *Minimum separable, under dark-adaptation, for subject 2.*

Large constellation (with minus 3.50D lens at eyepiece)			Small constellation (with minus 0.25D lens at eyepiece)	
Log I	Slit	Acuity (1/slit)	Slit	Acuity (1/slit×10)
Same as in Table 1.	1.6 mm	0.62	0.2	0.50
	2.8	0.36	0.4	0.25
	4.1	0.24	0.5	0.20
	4.6	0.21	0.6	0.16
	6.1	0.16	0.8	0.13
	6.4	0.15	0.9	0.11

large constellation. The anomaly, however, is not so marked between the two constellations as before. The difference between the two sets of curves is consistent with what is to be expected from the reversal

and balancing of disadvantages arising from the relative thicknesses of the glass lenses. In Fig. 1 acuity for the small constellation shows a general depression (corresponding to the use of a thick glass lens), and acuity for the large constellation shows a general elevation (corresponding to the use of a thin glass lens). In Fig. 2 acuity for the small constellation shows a general elevation (corresponding to the use of a thin glass lens), and acuity for the large constellation shows a general depression (corresponding to the use of a thick glass lens). These incidental differences between the two sets of curves are, however, of minor im-

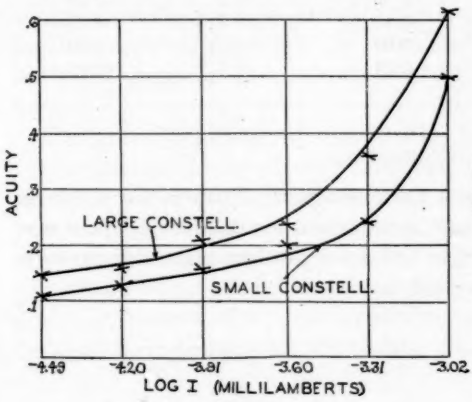

FIG. 2

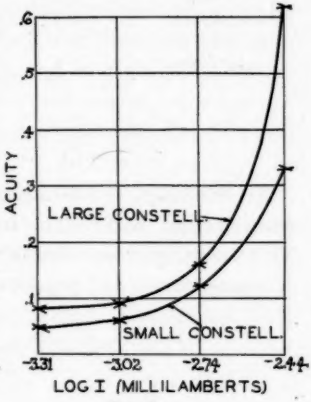

FIG. 3

FIG. 2. *Showing disparity in acuity between large and small constellations. Based on Table 2. As there is no overlapping between the two constellations, the curves represent definitely independent acuity functions. Crystalline maintained at the same accommodation for both constellations, approximately 3.50D, by the use of appropriate minus lenses.*

FIG. 3. *Showing disparity in acuity between large and small constellations. Based on Table 3. As there is no overlapping between the two constellations, the curves represent definitely independent acuity functions. Crystalline maintained at the same accommodation for both constellations, approximately 3.50D, by the use of appropriate minus lenses. Pupillary width maintained constant for both constellations by the use of an artificial pupil of 1 mm diameter, placed anteriorly to the lenses.*

portance when compared to the major circumstance that the anomaly persists despite the equalization of the crystalline to the same degree of accommodation for both constellations.

In the original investigation[4] the anomaly was found with a constant pupillary width for both constellations. Table 3 and Fig. 3 of the present work represent acuity values for simultaneous constant pupillary width (artificial pupil of 1 mm diameter) and constant accommodation (by

means of the same minus lenses as above) for both constellations. Here, too, the anomaly reappears.

TABLE 3. *Minimum separable, under dark-adaptation, with an artificial pupil of 1 mm diam., for subject 2.*

Large constellation (with minus 3.5D lens at eyepiece)			Small constellation (with minus 0.25D lens at eyepiece)	
Log I	Slit	Acuity (1/slit)	Slit	Acuity (1/slit×10)
−2.44369	1.6	0.62	0.3	0.33
−2.73612	6.4	0.16	0.8	0.13
−3.02855	11.7	0.09	1.6	0.06
−3.32098	12.8	0.08	1.7	0.05

CONCLUSION

An anomaly, consisting of a finer minimum separable for the large constellation than for the small, is confirmed for the dark-adapted eye. This anomaly is *not* a dioptrical artifact dependent upon differences in accommodation and pupillary width.

A MODIFIED BROCA PUPILLOMETER

By Frank K. Moss
[Lighting Research Laboratory, General Electric Company, Nela Park, Cleveland.
Received September 3, 1932]

Investigations of certain pupillary phenomena are frequently restricted because of the experimental difficulties encountered in measuring the pupil with precision. The photographic method employed by Reeves[1] to determine the relationship between illumination intensity and pupil size has the advantage of precision and the handicap of a somewhat elaborate experimental technique. Among the various pupillometers used or suggested, the characteristics of precision and simplicity of operation have seldom been combined in a practical instrument.

The type of pupillometer suggested by Broca[2] possesses the inherent characteristics of both precision and simplicity. In this instrument the diameter of the pupil is measured by the distance between two pinpoints of light so located and separated that the images of the pupil cast upon the retina appear tangential. The pupillometer is of the subjective, or perhaps better, of the intraocular type and hence lacks some of the desirable features of a purely objective instrument. The optical principles of the instrument are shown diagrammatically in Fig. 1.

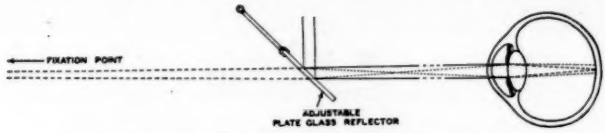

Fig. 1. *Illustrating the optical principles of the pupillometer.*

The actual instrument designed and used by the author is illustrated in Fig. 2. Essentially the pupillometer consists of a small mechanism so arranged that the distance between two points of light may be varied by means of a lead screw. This apparatus is attached to spectacle frames, directly in front of and at a distance of 6.6 centimeters from the right eye. The subject wears the instrument as ordinary eye glasses are worn, fixates upon a definite object and adjusts the distance between the two points of light until the retinal images appear tangential. The instrument is then removed from the head and the diameter of

[1] P. Reeves, *The Response of the Average Pupil to Various Intensities of Light*, J. Opt. Soc. Am., *4*, p. 35; 1920.

[2] Broca, C. R. Ac. Sci., *178*, p. 415; 1924. Couvreux, ibid, pp. 416 and 1388.

the pupil read on the graduated knob of the lead screw. The complete operation of adjusting and reading the instrument may be performed in a few seconds. Inexperienced subjects may be instructed in the opera-

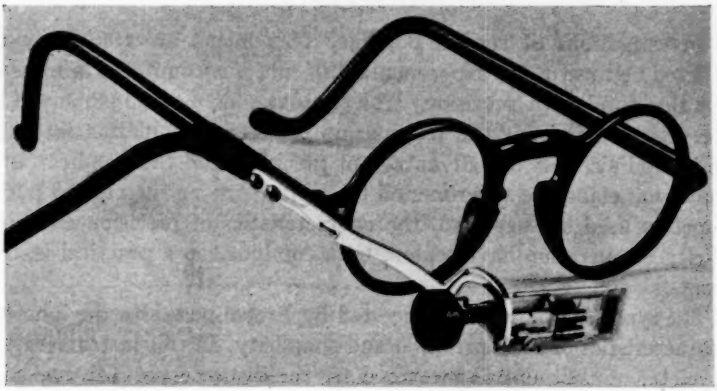

FIG. 2. *Showing the pupillometer proper and its position with respect to the right eye.*

tion of the instrument and acquire the ability to obtain reasonably consistent results within a period of a few minutes.

The two small points of light are formed by the intersection of a narrow slit, approximately 0.17 millimeters in width, in a fixed plate

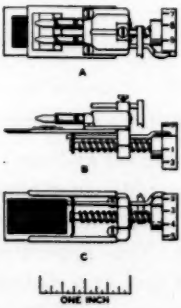

FIG. 3. *The mechanical details of the pupillometer. A shows the side farthest from the eye; B the top view; and C the side nearest the eye. In the illustration the width of the slits is exaggerated for clearness.*

and two inclined or V-shaped slits in a sliding plate. The mechanical features of the instrument are shown in detail in Fig. 3. The fixed slit and the movable V-shaped slits are clear lines on a heavy photographic

film developed to the deepest black. These slits were made with considerable nicety and precision by photographing a drawing which was enlarged twenty times. The intersections of the slits are illuminated by two frosted miniature lamps (Type T-3/4, 1.5 volts, 0.13 amp.), the bulbs of which are about the size and shape of a grain of wheat. The instrument proper, exclusive of the adjusting screw, is approximately 27 millimeters in length and 14 millimeters in width. Its weight, including the spectacle frames to which it is attached, is 29 grams.

The knob of the lead screw is calibrated in tenths of a millimeter, one complete revolution of the lead screw corresponding to one milli-

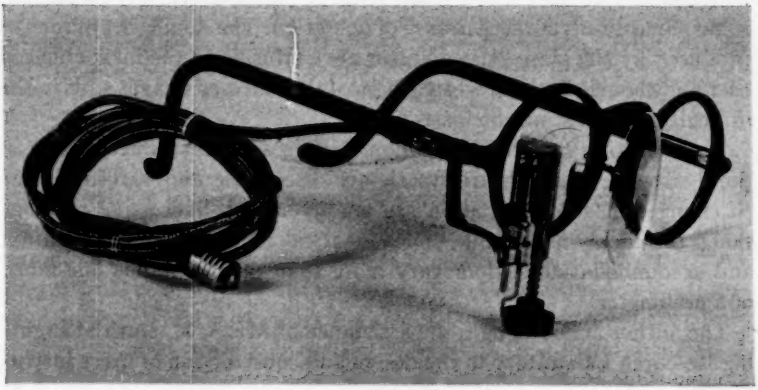

FIG. 4. *Showing a modification of the instrument illustrated in Fig. 2. In this design, the central visual field of the eye is not obscured by the mechanism of the pupillometer.*

meter in pupil diameter. A finer subdivision of the scale is unnecessary because of the comparatively wide momentary fluctuations in the size of the pupil. It is obvious that the instrument must be calibrated for a definite distance of the fixation-point from the eye. In the instrument shown in Fig. 2, this distance was taken as 1 meter. The slopes of the inclined slits are such that the pupillometer reads directly in millimeters for an accommodation of 1 meter. It is a simple matter to apply correction factors for various other fixational distances. The pupillometer, as constructed, has a range of 0–8 millimeters.

The instrument obscures a portion of the visual field of the right eye approximately 16° 40′ by 5° and 40′ in size. This is a recognized disadvantage of this type of instrument. However, since the light entering the totally exposed eye adds its pupillomotor influence to that entering

the other eye, the obscuring of a part of the central visual field of one eye is not a serious source of error in many researches. This is particularly true for investigations concerned only with the relative changes in pupil size. No attempt has been made to calculate the magnitude of the error introduced by the partial obscuring of the right eye.

Fig. 4 shows another form of pupillometer constructed to avoid the obscuring of the visual field. In this case the images of the two points of light are reflected into the right eye by means of a clear plate glass inclined at 45° to the line of vision. Although this type of pupillometer has the advantage of giving absolute (except for refraction at the cornea and aqueous humor) rather than relative measurements of pupil size, it has some disadvantages in ease of operation. The double set of images produced by the plate glass reflector are confusing to the inexperienced user and the relatively low brightness of the reflected images adds to the difficulty of adjusting the instrument.

The sensitivity of these pupillometers is such that fluctuations in pupil size due to the heart systole are discernible and variations due to changes in accommodation are readily noted. Successive readings taken as quickly as possible under identical conditions of illumination and accommodation seldom vary more than plus or minus one-tenth of a millimeter.

The author acknowledges the assistance of Mr. S. K. Guth of Lighting Research Laboratory in the design and construction of these instruments.

THE ABSORPTION AND DISPERSION OF CELLULOID BETWEEN 300A AND 1000A

By H. M. O'Bryan

[George Eastman Laboratory of Physics, Massachusetts Institute of Technology.

Received July 13, 1932]

ABSTRACT

The linear absorption coefficient of celluloid has been measured between 300A and 1000A and found to reach a maximum value of 1.1×10^6 per cm at 800A where a film 100A thick transmits 30 percent. The reflecting power of celluloid mirrors at various angles of incidence has been measured for six wave lengths in this region. From these reflection power curves and extinction coefficients, by using Fresnel's equations the refractive indices have been calculated for these wave lengths. The dispersion curve passes through unity at 800A, reaches a minimum at 550A and is approaching unity again at 400A. The total absorption between 300A and 3000A accounts for 126 electrons per molecule of cellulose nitrate. Exclusive of the K electrons of carbon, nitrogen, and oxygen, which show absorption near 40A, there are 192 electrons per molecule.

Introduction

Celluloid has long been recognized as a rather transparent substance over the entire range of the spectrum from the far infrared to the x-ray region. In addition, it is much easier to obtain in extremely thin films than any other common substance. Laird,[1] in 1920, examined the transmission of celluloid with a vacuum spectrograph and found that lines as short as 500A were transmitted. The films used were about 400A thick and showed progressively increasing opacity toward shorter wave lengths. Using the general radiation excited by electron impact, Holweck[2] measured the absorption coefficients from the x-ray region to about 900A. He found that the mass absorption coefficient reached a maximum of 10^5 per g per cm^2 at 300A, while the experiments of the author give values which are several times larger at 300A and reach a maximum at 800A. The great differences noted may be due to variations in the constitution of the celluloids used but are more probably caused by the lack of monochromatic radiation in Holweck's experiments. Neufeldt[3] has examined the transmission of celluloid between 17A and 51A with a Geiger counter and monochromatic radiation. The absorption of the K electrons of carbon, nitrogen, and oxygen resemble optical absorption rather than the λ^3 law of x-ray absorption.

The combination of reflection and absorption measurements in the

[1] E. R. Laird, Phys. Rev., *15*, 543; 1920; Phys. Rev., *29*, p. 41; 1927.

[2] F. Holweck, *De La Lumiere Aux Rayons X*, p. 70.

[3] H. Neufeldt, Zeits. f. Physik, *68*, p. 659; 1931.

present experiments gives values which are consistent with both Fresnel's equations of reflection and dispersion theory. While the magnitude of the absorption causes some experimental difficulty, the factor which has previously delayed studies of this kind has been lack of sufficient intensity even for photographic measurements in this region.

SPECTROGRAPH AND SOURCE

The vacuum spectrograph and source are much the same as described in a previous article[4] but a few slight improvements seem worth mentioning. A side tube T shown in Fig. 1a was added to permit the introduction of the absorbing films between the slit and grating. An elec-

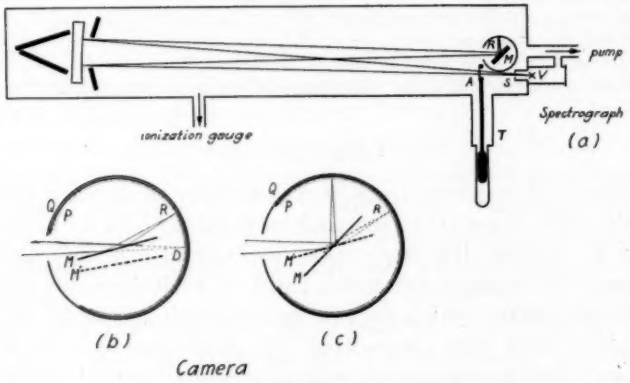

FIG. 1. *Spectrograph and camera.*

tromagnet was used to move the film carrier in and out of the light beam without disturbing the vacuum. As many as four absorbing films could be held on the carrier at A and examined on one photographic film. Figs. 1b and 1c show the camera for holding photographic films for either reflection or absorption. The concentric cylinders P and Q could be rotated with respect to each other so that there was no necessity for darkening the room when the camera was inserted in the spectrograph. The front of the cylinder P was open about 80° permitting 20 exposures of the unreflected beam to be taken on one photographic film. The grating was adjusted so that a wire of one millimeter diameter on the axis of the camera divided the spectrum symmetrically from the central image to 1000A. This permitted the reflection of all wave lengths simultaneously at the same angle of incidence.

[4] H. M. O'Bryan, Phys. Rev., *38*, p. 32; 1931.

The back of the glass grating was ground and polished at an angle of 4° with the optical axis. This prevented any of the light from the back glass surface (about 4 percent of the visible light) from reaching the photographic film. The spectra now seem almost completely free from scattered light except that scattered by the rulings themselves which was very faint with the glass grating used.

The "hot spark" source is sufficiently steady and although less than one kilowatt of power was put into it, the exposure times are as short as one can time readily. Just which factors are responsible for the improvement are unknown. It is hoped that experiments can be made with an element whose spectra are better classified to ascertain the ef-

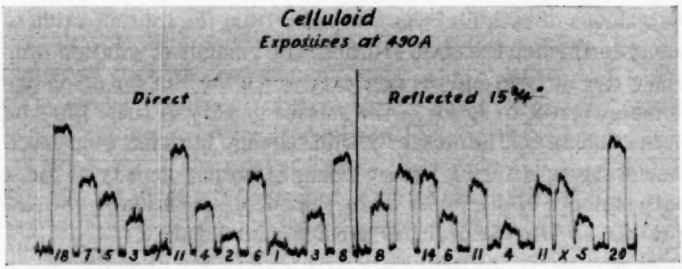

FIG. 2. *Sample photometer curve.*

fects of capacity, inductance, voltage and frequency. The condenser consisted of enough aluminum plates in a glass battery jar filled with oil to make a capacity of 500 cm.

The frequency of the spark discharge was about 5×10^6 (wave length 60 meters). The spark was operated every four seconds for one-quarter second, from a time several minutes before the first exposure began until the series of exposures on one photographic film were finished. The insertion of the absorbing film or mirror and the turning of the mirror or photographic film was accomplished during the intervals between spark discharges. The numbers at the base of the photometer curve in Fig. 2 are the number of these one-quarter second flashes for the particular exposure.

THE CELLULOID FILMS AND MIRRORS

The celluloid on which the numerical results are reported was one used for photoelastic studies and was quite transparent to visible light. The density of the solid was 1.4 and refractive index for visible light

1.65. It was composed chiefly of cellulose nitrate with some camphor or similar material added to improve the mechanical properties. The constitution $C_{12}H_{16}O_6(NO_3)_4$ was taken for computation of the molecular weight and the number of absorbing electrons due to the various atoms. This estimate of the carbon, nitrogen, oxygen, and hydrogen content seems sufficiently accurate in view of the experimental uncertainties involved. Three other samples of commercial celluloids and cellulose acetate gave absorption of about the same magnitude and location.

The films from which the absorption measurements are taken were made by dropping a dilute amyl acetate solution of celluloid on a water surface and removing small portions of the film on aluminum frames. The thickness of each film was computed from the concentration of the celluloid in the amyl acetate solution, the amount of solution dropped on the water surface, and the area over which the film spread on drying. It is more correct to speak of the surface density of these films rather than the thickness. The density of thin celluloid films has been described by one observer[5] as being almost twice the normal density of the solid. In each instance in this paper where thickness is mentioned, the equivalent thickness with the ordinary density is intended.

Films of from 60A to 400A thick were used for the numerical measurements and were "black" by reflected light. The degree of "blackness" was always in qualitative agreement with the computed thickness and quantitative measurements of the transmission of visible light by these films might prove a fair index of their thickness. Films thick enough to show any colors by reflected light completely absorbed all energy between 300A and 1000A.

To detect any influence of the amyl acetate or water on the ultraviolet absorption several films made from an ethyl alcohol and ether solution of celluloid dropped on a mercury surface were examined. It was not possible to obtain these as thin as those from a water surface but they showed absorption of the same magnitude and location in the ultraviolet.

The thinnest celluloid films deteriorated after several days in a high vacuum or a few weeks in air. It was very rarely that a film was broken by a "projectile" from the hot spark so the yield of successful absorption photographs was rather high. The actual absorbing area of each film was 4 mm $\times$ 6 mm.

[5] E. R. Laird, Phys. Rev., *19*, p. 384; 1922.

The mirrors for the reflection measurements were made by flowing celluloid solution on a piece of carefully levelled plate glass. After evaporation of the amyl acetate solution the celluloid was about one-hundredth of a millimeter thick. These mirrors had a figure almost as good as selected plate glass and a surface of high quality.

PHOTOGRAPHIC METHODS

In all this work the reciprocity law has been assumed and comparison exposures made by varying the exposure times. It is quite possible to use mesh screens with a collimating mirror at about 15° from grazing incidence by doubling the exposure times and thus avoid the necessity of making this assumption, but this is not readily accomplished for mechanical reasons. Oiled films were used entirely. The step exposures were made both before and after the absorption or reflection exposures and adjacent to them. The spectral image of each line was 1.5 mm×0.7 mm and under proper adjustment of the spark electrodes gave "flat topped" photometer curves as shown in Fig. 2. This curve is for wave length 480A, one of the weaker lines of the source and shows a number of exposures of the direct beam and those reflected at 15¾° from grazing incidence from a celluloid mirror. Often the slit was not uniformly illuminated and the photometer curve showed characteristic irregularities which were identical in both direct exposures and through the celluloid films. Such irregularities on reflection were the same as in the direct beam except reversed from right to left by the reflection. The photographic definition was not impaired either by the absorption or reflection.

The reflection measurements were made in two parts: (1) comparison of reflections at 15¾° with the direct beam (Fig. 1b); (2) comparison of reflections at angles from 3° to 80° to those at some angle about 15° (Fig. 1c).

From part 2 a curve of reflecting power against angle of incidence was drawn which was relative to the reflecting power at 15°. Then by the absolute reflecting power at 15¾° obtained from part one the entire curve from part two was reduced by the factor necessary to make the reflecting power at 15¾° equal its absolute value. This eliminated an obvious weakness in earlier measurements[4] where the reflection at 1½° was taken as 100 percent.

A method of obtaining the optical constants of a solid without the assumption of any photographic law is suggested by Fig. 1a. For an absorbing film which transmits more than is reflected from the same substance at normal incidence there is always one angle of incidence

at which the percentage of incident energy reflected is equal to that transmitted by the film. For a given exposure time if the angle of incidence which gives the same photographic blackening as the absorption is found, then by means of the thickness of the absorbing film and Fresnel's equations of reflection and absorption, the reflecting power and extinction coefficient can be calculated. This method requires such accurate measurement of the thickness of the absorbing film and long calculations as to render it impractical.

CALCULATION OF THE REFRACTIVE INDEX AND EXTINCTION COEFFICIENT

The photometer curves of the absorption photographs give the percentage transmission of the celluloid films and the linear absorption coefficient μ can be computed from the formulae

$$I = I_0 \epsilon^{-\mu x} \tag{1}$$

where x is the film thickness. The normal density of celluloid is taken for the thin films. From the value of the reflecting power at normal incidence it was possible to correct for the reflection at the surfaces of the absorbing film. As the maximum reflecting power at normal incidence was about 10 percent these corrections were not large and were within the experimental error. It is difficult to make a rigorous calculation of these corrections for the films are not thick enough to give the full reflection expected when the thickness is many times the wave length of light. The extinction coefficient x is then given by

$$4\pi x/\lambda = \mu. \tag{2}$$

Table 1 shows the average values of μ and x as determined from seven celluloid films from 60A to 600A thick. The wave lengths are those of some of the stronger tungsten lines. It is hoped that these points are within 25 percent of their absolute value, and believed that the relative wave length accuracy is much greater.

The reflection measurements gave a set of curves at the same tungsten wave lengths for the reflecting power against the angle from grazing incidence. Each of these curves permits a calculation of both the refractive index η and extinction coefficient x from Fresnel's equations from electromagnetic theory. The general form for reflection from an absorbing medium given by König[6] was taken

$$R = \frac{b^2 + (a - \sin\theta)^2}{b^2 + (a + \sin\theta)^2} \cdot \frac{b^2 + a^2 + \cos\theta^2 \cot^2\theta}{b^2 + (a + \cos\theta \cot\theta)^2} \tag{3}$$

[6] W. König, Handb. d. Physik, *XX*, p. 242.

where

$$a^2 = \tfrac{1}{2}[(\{\eta^2(1-x^2) - \cos^2\theta\}^2 + 4\eta^4x^2)^{1/2} + \eta^2(1-x^2) - \cos^2\theta]$$
$$b^2 = \tfrac{1}{2}[(\{\eta^2(1-x^2) - \cos^2\theta\}^2 + 4\eta^4x^2)^{1/2} - \eta^2(1-x^2) + \cos^2\theta]$$

where R = reflecting power and θ = angle from grazing incidence.

This form of Fresnel's equation applies only to unpolarized incident light. The light incident on the mirrors in this experiment is diffracted by the grating and from observations on gratings in the visible and infrared regions, it is probably partially polarized. To simplify the calculations it is assumed that the light is unpolarized and again it is hoped that the errors involved are not large.

TABLE 1. *Refractive index η, extinction coefficient x, linear absorption coefficient μ and percentage transmission of a celluloid film 100A thick.*

Angstroms	η	x	$\mu\times10^{-6}$	Percent transmission
300		0.09	0.37	79
388	0.85	0.18	0.58	55
480		0.29	0.77	45
554	0.80	0.38	0.87	42
648		0.46	0.89	39
686	0.90	0.53	0.93	37
770	1.00	0.65	1.05	33
843		0.73	1.09	30
885	1.15	0.75	1.07	32
1000	1.10	0.79	1.00	35
2150			0.05	
2260			0.01	

As the Eqs. (3) suggest, it is a very laborious calculation to obtain both η and x by finding the curve which fits the experimental data. It is much easier to insert x as found from the direct measurement of absorption in the equations and try a number of values of η until a satisfactory fit of the experimental reflecting power is obtained for each wave length. The type of agreement found for 388A is shown in Fig. 3. At this wave length $x^2 = 0.05$ was sufficiently close to the experimental value of 0.033 to show that neither $\eta = 0.9$ nor 0.8 were as satisfactory as 0.85. In Fig. 3 two values of x^2 are plotted and we see that a value near 0.05 is more satisfactory. Curves of the same type were calculated for six wave lengths to determine η and check the experimental value of x. For angles near the normal the experimental reflecting powers are not to be trusted too much as the reciprocity law is known to be most

unsatisfactory when the intensities compared differ by a large factor. The reflecting power at normal incidence may also be influenced by surface roughness of the mirror. From the depolarization of visible light

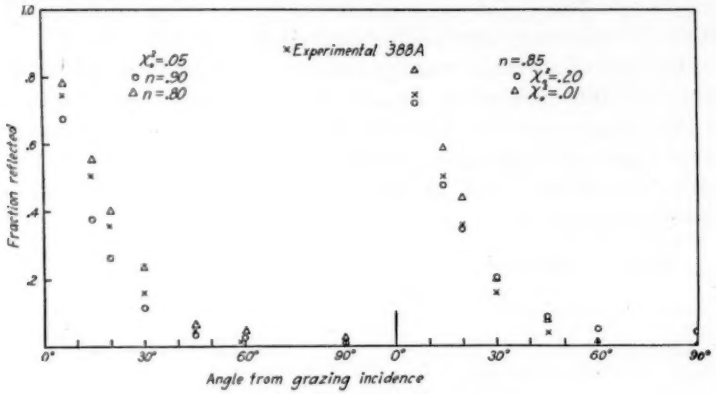

FIG. 3. *Calculation of the refractive index.*

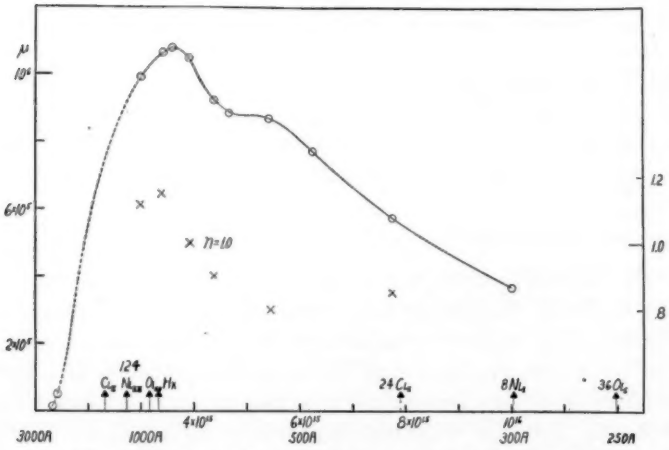

FIG. 4. *Linear absorption coefficient and refractive index of celluloid.*

reflected at Brewster's angle from glass the transition layer is found to be from 10A to 50A thick. This means that wave lengths less than ten times this surface layer will not follow Eqs. (3) at normal incidence. In the calculations of η the reflecting power between 0 and 45° has been fitted more closely. When the refractive index exceeds unity more ac-

curate experimental data are required for the same accuracy in η. The values of η in Table 1 may be off as much as 0.05, especially above 800A.

The calculations, however, are sufficiently positive to show that η passes through unity at about 800A, reaching a minimum of about 0.8 and approaching unity again at shorter wave lengths. This agrees with observations in the x-ray region. At 554A the external critical angle for total reflection would be 35° if the absorption were absent. In spite of the tremendous absorption the influence of the refractive index is still large for it is x rather than μ which is important. In Fig. 4 η and μ are plotted against the frequency and in general resemble the ordinary absorption and dispersion curves.

DISCUSSION

Fortunately celluloid is composed of hydrogen and three other light atoms which are adjacent to each other in the periodic table. By assuming that the celluloid is composed entirely of cellulose nitrate $C_{12}H_{16}O_6(NO_3)_4$ the number of electrons in each of the K and L shells has been computed and listed in Table 2. The absorption edges listed have been

TABLE 2. *Absorption edges and number of electrons f for each K and L shell per molecule of* $C_{12}H_{16}O_6(NO_3)_4$.

Atoms	16 H	24 C			4 N			18 O		
Shell	K	K	L_{I}	$L_{\text{II-III}}$	K	L_{I}	$L_{\text{II-III}}$	K	L_{I}	$L_{\text{II-III}}$
λA	910	45	380	1300	36	300	1100	25	250	950
f	16	24	24	24	8	8	12	36	36	72

obtained[7] from soft x-ray and critical potential methods so do not show exactly what should be observed for the same atoms combined to form celluloid. Neufeldt[3] has measured the K absorption of C, N and O in celluloid and found their positions to coincide with the values listed in Table 2.

Kronig[8] has shown that the number of absorbing electrons per atom f can be expressed in terms of the total atomic absorption coefficient α by the formulae

$$f = (mc/\pi e^2)\alpha \tag{4}$$

where α is defined by $N\alpha = \int \mu d\nu$ and N is the number of atoms per cubic centimer. In the present case it is more suitable to use f as the number of

[7] A. H. Compton, *X-Rays and Electrons*, p. 190; 1927.
[8] R. deL. Kronig, J. Opt. Soc. Am., *12*, p. 547; 1926.

electrons per molecule of cellulose nitrate and N as the number of molecules per cubic centimeter. This gives the formulae for f in terms of the measured linear absorption coefficient

$$f = (mc/\pi Ne^2) \int \mu d\nu. \tag{5}$$

By graphical integration of μ in Fig. 4, f is found to be 107 electrons per molecule between 1000A and 300A. The same method gives 19 for the region between 3000A and 1000A. The dotted line is simply drawn to connect the points near 2000A determined with a quartz spectrograph and those near 1000A. There are 70 electrons per molecule unaccounted for by this calculation. While some of these are below 300A the interpolated and experimental values of μ are not accurate enough to say how many. The location of the K, L_{I} and $L_{\text{II-III}}$ absorption edges given in Table 2 are indicated in Fig. 4.

The contribution of these electrons to the refractive index for the frequency ν_0 can be computed by the formulae[9]

$$\frac{\eta^2 - 1}{\eta^2 + 2} = \frac{c}{3\pi^2} \int \frac{\mu}{\nu^2 - \nu_0^2} d\nu. \tag{6}$$

A graphical integration over the region from 300A to 3000A gave $\eta = 1.73$ for 6000A while the refractive index for visible light was measured to be 1.65. The computed value of the refractive index at 6000A depends almost equally on the absorption measured below 1000A and that above 1000A as found by interpolation. The influence of the absorption below 300A is expected to be quite small. A similar integration would determine the refractive index for frequencies within the region of absorption but as the integrand of Eq. (6) becomes infinite at $\nu = \nu_0$ graphical integration is not easy. A very crude calculation gave fair agreement with the values shown in Table 1.

Further experiments are being made to obtain the absorption of metallic elements on celluloid films and to extend these measurements to shorter wave lengths. It is also hoped that the celluloid will prove useful as windows for gas absorption cells. The measurements reported here were started at the Johns Hopkins University, and the spectrograph used was obtained from there through the kindness of Professor R. W. Wood.

[9] K. L. Wolf and K. F. Herzfeld, Handb. d. Physik, *XX*, pp. 480–634.

OPTICAL SOCIETY OF AMERICA

STATEMENT OF CASH RECEIPTS AND DISBURSEMENTS

For the Period from January 1, 1931 to December 31, 1931

Cash on Hand, January 1, 1931		$ 3,860.93
Receipts:		
Membership dues arrears, 1930	$ 40.00	
Membership dues current, 1931:		
1931 dues, total collected in 1930 and 1931	5,014.90	
1931 dues, total collected prior to Jan. 1, 1931	2,960.30	
1931 dues, total collected Jan. 1, 1931–Dec. 31, 1931	2,054.60	
Membership dues in advance 1932	2,632.50	
Subscriptions to support of society	3,000.00	
Interest on bank balances	106.24	
Interest on bonds	832.50	
Interest on bonds (Ives Fund) (500 lib. 4¼'s)	21.25	
Share of society in Journal subscriptions	215.60	
Share of society from Advertisements in journal	200.00	
Sales of back numbers, Vols. I–V (Property of Society)	137.30	
Total receipts		$ 9,239.99
TOTAL RECEIPTS PLUS CASH ON HAND, JANUARY 1, 1931		$13,100.92
Disbursements:		
To Journal of the Optical Society of America and the Review of Scientific Instruments as per agreement with Association of Scientific Apparatus Makers	$ 4,800.00	
Journal subscriptions (318 at $3.00 each)	954.00	
Printing and stationery	634.90	
Postage and telegraph in connection with business of society	133.43	
Postage, back numbers of Journal	1.72	
Travelling on business of society	96.41	
Clerical expenses	157.09	
Fire insurance Vols. I–V	6.80	
Labor and transportation on addressograph	115.11	
Sundry expense, treasurer	63.53	
Ives Medal expense	17.18	
Total disbursements		$ 6,980.17
Cash on hand, Dec. 31, 1931		6,120.75
TOTAL DISBURSEMENTS PLUS CASH ON HAND, DECEMBER 31, 1931		$13,100.92

Investments:

$ 7,000 Atchison, Topeka and Santa Fe Gen. 4's
$13,000 Fourth Liberty 4¼'s
$ 500 Fourth Liberty 4¼'s (Frederick Ives Medal Endowment Fund)

I certify that the above report is correct to the best of my knowledge and belief.

(*signed*) ADOLPH LOMB, *Treasurer*

February 6, 1932.

ADOLPH LOMB, ESQ.,
TREASURER, OPTICAL SOCIETY OF AMERICA:
DEAR MR. LOMB,

In accordance with your request we have audited the Treasurer's ac-

counts of the Optical Society of America for the twelve months ending December 31, 1931: and we hereby certify that the Treasurer's official report of receipts, disbursements and investments for the year 1931 is correct in every detail, as shown by bank statements, vouchers, etc.

Yours truly,

(*Signed*) JAMES P. C. SOUTHALL
C. L. TRELEAVEN

INDEX TO VOLUME 22

("A" designates abstract of paper presented before the Optical Society.)

A

Abbe refractometer, limitations of a blanket calibration chart for reading dispersions on the (Laurence Ellsworth Dodd), 477.
Absorption by metals, plane waves of light, III (T. C. Fry), 307, 434-A.
Accommodation, pupillary width, and stimulus distance (Ellis Freeman), 729.
Aerial cameras, (C. H. Birdseye), 137.
——— mapping, brock process of (Edward H. Cahill), 111.
——— photographic mapping, 4.
——— stereo-photographic mapping instruments and methods (C. H. Birdseye), 137.
Allen, A. J. and R. G. Franklin: The sensitization of ordinary photographic plates to wave lengths below 2500A, 469.
Amendment to by-laws, 424
American Institute of Physics, 3.
Appointment of representatives in, 424.
Ames, A., Jr., Kenneth N. Ogle and Gordon H. Gliddon: Corresponding retinal points, the horopter and size and shape of ocular images, Part I, 538: Part II, 575.
Amplification of small voltages, special tubes for the (G. F. Metcalf), (Title only), 423.
Annual meeting of the Optical Society of America, Proceedings of the, 1.
———, Place for 1932, 425.
Anomalies of visual acuity in relation to stimulus-distance (Ellis Freeman), 285.
Appleyard, E. T. S. and J. J. Hopfield: A simplified method of preparing Schumann plates, 488.
Associate editors, appointment of, 424.
Astronomy, photographic plates for use in spectroscopy and, II (C. E. Kenneth Mees), 204, 427-A.
Atmosphere, The ultraviolet transmission coefficient of the earth's (R. S. Rockwood and R. A. Sawyer), 513.
Automatic optical control, a bolometer for (K. Hickman and C. R. Sanford), 13-A.
Average eye, trichomatic functions of the (W. F. Hamilton and Ellis Freeman), 369.

B

Barbrow, L. E., F. R. Caldwell and W. F. Roeser: Photometric standards based on a black body at the freezing point of iridium, 7-A.
Bauer, Simon H.: Function of sin x/x, 537.
Bench for testing photographic lenses, a new (R. Kingslake) 13-A; 207.
Bennett, Harold F.: Differences in path length through a lens in terms of its reciprocal spherical aberration, 14-A.
Birdseye, C. H.: Aerial stereo-photographic mapping instruments and methods, 137.
Black body immersed in freezing iridium, applications to photometry of a (H. T. Wensel), 433-A.
Bolometer for automatic optical control, (K. Hickman and C. R. Sanford), 13-A.
Broca pupillometer, a modified (Frank K. Moss), 735.
Brock process of aerial mapping (Edward H. Cahill), 111.
Business office of the Journal of the Optical Society of America, transfer of, 425.

C

Cahill, Edward H.: Brock process of aerial mapping, 111.
Caldwell, F. R., Wm. F. Roeser and L. E. Barbrow: Photometric standards based on a black body at the freezing point of iridium, 7-A.
Calibration chart for reading dispersions on the Abbe refractometer, limitations of a blanket (Laurence Ellsworth Dodd), 477.
Cambridge meeting of the Optical Society of America, 422.
Camera and stereoscope for orthostereoscopic pictures at magnifications from unity to 24×, (H. F. Kurtz), 18-A.
Cando-luminescence, on temperature crests in (E. L. Nichols and H. L. Howes), 170.
Cash Receipts and Disbursements, Journal of the Optical Society of America; The Review of Scientific Instruments, 435.
Celluloid, absorption and dispersion of, between 300A and 1000A (H. M. O'Bryan), 739.
Chromatic fields as a function of wave length, retinal (Charles A. Rinde), 333.
Chromaticity sensibility to stimulus differences (Deane B. Judd), 72.
Coiled filaments in incandescent lamps, characteristics of (Gordon R. Fonda and Arthur A. Vernon), 223.
Color blindness test of more than 6500 persons, note on a (I. H. Godlove), 430-A.
Color Council, organization of the Inter-Society, 5.
Color, a method of projection in relief and (Herbert E. Ives), 191.
———, projection in relief and (H. E. Ives), 17-A.
——— temperature, chromaticity sensibility to temperature change as a function of (Deane B. Judd), 9-A.
——— temperature determinations of incandescent lamps, investigation of sources of errors in (Deane B. Judd), 429-A.
——— temperature, nearest, for stimuli yielding non-Planckian but nearly achromatic colors, 428-A.

Colorimeter, a trichromatic (J. Zernike), 418.
Colorimetric purity, a general formula for the computation of (Deane B. Judd), 10-A.
Colorimetry, the applicability of photoelectric cells to photometry and (Arthur C. Hardy and O. W. Pineo), 427-A.
——— committee of the International Commission on Illumination and the actions taken at the meeting in Cambridge, England, September, 1931, report on the work of (Irwin G. Priest), 431-A.
Committee on photographic standard of intensity, report of, 16.
Committees appointed by President, 424.
Concave grating spectrograph, especially at large angles of incidence, (J. E. Mack, J. R. Stehn, and Bengt Edlen), 245.
CONDON, E. U., and F. SEITZ: Lorentz double refraction in the regular system, 393.
CRITTENDEN, E. C.: Progress toward international agreement on photometric standards, 433-A.

D

Daylight into the sea, on the penetration of (E. O. Hulburt), 408.
DEBYE, P.: Interferometric measurements on single molecules, (title only) 423-A.
Densitometer for spectrograms, measuring microscope and (Gustave Fassin), 13-A.
"Depressed" beam of motor car headlight (L. W. Taylor), 65.
Digitalis, influence of ultraviolet rays on pharmacological potency of (David I. Macht), 16-A.
DODD, LAURENCE ELLSWORTH: Limitations of a blanket calibration chart for reading dispersions on the Abbe refractometer, 477.
Double refraction in the regular system, Lorentz (E. U. Condon and F. Seitz), 393

E

Earth's atmosphere, the ultraviolet transmission coefficient of the (R. S. Rockwood and R. A. Sawyer), 513.
EASLEY, M. A. and W. E. FORSYTHE: A method of measuring the maximum intensity of light of the photoflash lamp or other source of short duration, 6-A.
Eclipse projector for the Franklin Institute museum, (James Stokley), 239.
Editorial. The retirement of Dr. Paul D. Foote as Editor-in-Chief, 467.
EDLÉN, BENGT, J. E. MACK, and J. R. STEHN: On the concave grating spectrograph, especially at large angles of incidence, 245.
Electronic devices and their applications to research, joint symposium on, (title only), 423.
——— as aids to research, (A. W. Hull), (title only), 423.
———, some practical applications of (N. P. Rashevsky), (title only), 423.
Elliptic polarization of light by total internal reflection (W. W. Sleator), 15-A.
EWER, MARY A. and E. L. NICHOLS: Thermal behavior of certain solid solutions, 456.

F

FASSIN, GUSTAVE: Measuring microscope and densitometer for spectrograms, 13-A.
Financial statement, J.O.S.A.-R.S.I , 435
Fog and haze, transmission of light by (F. M. E. Holmes and Brian O'Brien), 9-A.
FONDA, GORTON R. and ARTHUR A. VERNON: Characteristics of coiled filaments in incandescent lamps, 223.
Foote as Editor-in-Chief, the retirement of Dr. Paul D. Editorial, 467.
FORSYTHE, W. E. and M. A. EASLEY: A method of measuring the maximum intensity of light of the photoflash lamp or other source of short duration, 6-A.
Franklin Institute Museum, An eclipse projector for the (James Stokley), 239.
FRANKLIN, R. G. and A. J. ALLEN: The sensitization of ordinary photographic plates to wave lengths below 2500A, 469.
FREEMAN, ELLIS: Accommodation, pupillary width, and stimulus distance, 729.
———, Anomalies of visual acuity in relation to stimulus-distance, 285.
———, Intensity, area, and distance of visual stimulus, 402.
——— and W. F. HAMILTON: Trichromatic functions of the average eye, 369.
FRY, THORNTON C.: Plane waves of light, III. Absorption by metals, 307, 434-A.

G

GARDNER, I. C.: An attachment for producing approximately spherical surfaces of small curvature on a lathe, 432-A.
Glass, relation between the composition and the density and optical properties of. I. The soda-lime-silica glasses. (G. W. Morey and H. E. Merwin), 632.
GLIDDON, GORDON H., A. AMES, JR. and KENNETH N. OGLE: Corresponding retinal points, the horopter and size and shape of ocular images. Part I, 538; Part II, 575.
GODLOVE, I. H.: Standardization of Munsell colors, 429-A.
———, Note on a color blindness test of more than 6500 persons, 430-A.
DE GRAMONT, ARMAND: The influence of surface polish upon the light transmitted in "total" reflexion, 11-A.
Grating spectrograph, especially at large angles of incidence, on the concave (J. E. Mack, J. R. Stehn, and Bengt Edlén), 245.
Gratings, the use of plane transmission (H. M. Reese), 496.

H

HAMILTON, W. F. and ELLIS FREEMAN: Trichromatic functions of the average eye, 369.

HARDY, ARTHUR C. and O. W. PINEO: The applicability of photoelectric cells to photometry and colorimetry, 427-A.
———, The computation of trichromatic excitation values by the selected ordinate method, 430-A.
Haze, transmission of light by fog and (F. M. E. Holmes and Brian O'Brien), 9-A.
HENNING, F. and H. T. WENSEL: The freezing point of iridium, 7-A.
HICKMAN, K. and C. R. SANFORD: A bolometer for automatic optical control, 13-A.
High-voltage transformers for x-ray work, note on, 238.
HOLMES, F. M. E. and BRIAN O'BRIEN: Transmission of light by fog and haze, 9-A.
HOPFIELD, J. J. and E. T. S. APPLEYARD: A simplified method of preparing Schumann plates, 488.
Horopter and size and shape of ocular images, corresponding retinal points, Part I (A. Ames, Jr., Kenneth N. Ogle and Gordon H. Gliddon), 538 Part II, 575.
——— analytical treatment of the longitudinal; its measurement and application to related phenomena, especially to the relative size and shape of the ocular images (Kenneth N. Ogle), 665.
HOWES, H. L. and E. L. NICHOLS: On temperature crests in cando-luminescence, 170.
HULBURT, E. O.: On the penetration of daylight into the sea, 408.
HULL, A. W.: Electronic devices as aids to research, (title only), 423.
HUMPHREYS C. J., W. F. MEGGERS and C. C. KIESS: Infrared spectrum photography, 428-A.

I

Illumination in spectrographs, on the intensity of (O. Oldenberg), 441.
Incandescent lamps, characteristics of coiled filaments in (Gorton R. Fonda and Arthur A. Vernon), 223.
———, Investigation of sources of errors in color temperature, determinations of (Dean B. Judd), 429-A.
Incorporation of the Optical Society, 425.
Interference fringes of equal slope in polarized light, photographs of the Lummer "doubling" of (Reinhard A. Wetzel), 14-A.
Interferometer method of studying the vibrations of an oscillating quartz plate (Harold Osterberg), 19.
Interferometric measurements on single molecules (P. Debye), (title only), 423-A.
Internal reflection, the elliptic polarization of light by total (W. W. Sleator), 15-A.
International agreement on photometric standards, progress toward (E. C. Crittenden), 433-A.
Intersociety Color Council, 426.
———, appointment of representatives on, 424.
———, organization of the, 5,
———, report from representatives of the Optical Society in, and discussion of the report, 431-A.
Infrared, a universal spectrometer for the (A. H. Pfund), 281.
———, spectrum photography (W. F. Meggers, C. C. Kiess and C. J. Humphreys), 428-A.
Iridium, applications to photometry of a black body immersed in freezing (H. T. Wensel), 433-A
———, the freezing point of (F. Henning and H. T. Wensel), 7-A
———, photometric standards based on a black body at the freezing point (F. R. Caldwell, Wm. F. Roeser and L. E. Barbrow), 7-A.
IVES, FREDERICK E.: Polychrome photography, 199.
IVES, HERBERT E : A method of projection in relief and color, 191.
———, Projection in relief and color, 17-A.
Ives medal to Professor Theodore Lyman, award of, 2.

J

JAMES, LOUIS E. and FRANKLIN E. POINDEXTER: Effect of intensity and underlying fogs on the latent image, 525.
Journal of the Optical Society of America, Statement of Cash Receipts and Disbursements, 435.
JUDD, DEANE B.: Chromaticity sensibility to temperature change as a function of color temperature, 9-A.
———, Chromaticity sensibility to stimulus differences, 72.
———, A general formula for the computation of colorimetric purity, 10-A.
———, Investigation of sources of errors in color temperature determination of incandescent lamps, 429-A.
———, Nearest color temperature for stimuli yielding non-Planckian but nearly achromatic colors, 428-A.

K

KIESS, C. C., C. J. HUMPHREYS and W. F. MEGGERS: Infrared spectrum photography, 428-A.
KINGSLAKE, R.: A new bench for testing photographic lenses, 13-A, 207.
KNOWLES, T. and A. H. TAYLOR: The interpretation of spectrograms, 229.
KURTZ, H. F.: A camera and stereoscope for orthostereoscopic pictures at magnifications from unity to 24×, 18-A.

L

Latent image, the effect of intensity and underlying fogs on the (Franklin E. Poindexter and Louis E. James), 525.
Limitations of a blanket calibration chart for reading dispersions on the abbe refractometer (Laurence Ellsworth Dodd), 477.
Lomb, Adolph, Memorial, 663.
Lorentz double refraction in the regular system (E. U. Condon and F. Seitz), 393.
LOVELAND, R. P.: An apparatus for motion photomicrography with 35 mm film, 18-A, 161.
Luminescence, the relation between certain types of (E. L. Nichols and Frances G. Wick), 15-A, 357.
Lummer "doubling" of interference fringes of equal slope in polarized light, photograph of the (Reinhard A. Wetzel), 14-A.
Lyman, Theodore, Award of Frederic Ives medal to, 2.

M

MACHT, DAVID I.: Influence of ultraviolet rays on pharmacological potency of digitalis, 16-A.
MACK, J. E., J. R. STEHN, and BENGT EDLÉN: On the concave grating spectrograph, especially at large angles of incidence, 245.
Maximum intensity of light of the photoflash lamp or other source of short duration, a method of measuring the (W. E. Forsythe and M. A. Easley), 6-A.
Measuring microscope and densitometer for spectrograms (Gustave Fassin), 13-A.
MEES, C. E. K.: Photographic plates for use in spectroscopy, 17-A.
———, Photographic plates for use in spectroscopy and astronomy II, 204, 427-A.
MEGGERS, W. F., C. C. KIESS and C. J. HUMPHREYS: Infrared spectrum photography, 428-A.
MERWIN, H. E. and G. W. MOREY: Relation between the composition and the density and optical properties of glass. I. The soda-lime-silica glasses, 632.
METCALF, G. F.: Special tubes for the amplification of small voltages, (title only), 423.
Michelson, A. A., Tribute to, 2.
MILLER, ORAN E.: Wedge spectrograms without an absorbing wedge, 13-A.
Molecular shape and orientation in liquids (C. P. Smyth), (title only), 423-A.
Molecules, interferometric measurements on single (P. Debye), (title only), 423-A.
MOREY, G. W. and H. E. MERWIN: Relation between the composition and the density and optical properties of glass. I. The soda-lime-silica glasses, 632.
MOSS, FRANK K.: A modified Broca pupillometer, 735.
Motion photomicrography with 35 mm film, an apparatus for (R. P. Loveland), 18-A, 161.
Motion picture industry, optical problems of the, 2.
——— projection from continuously moving film, the problem of (Fordyce Tuttle and Chas. D. Reid), 39.
Motor car headlight, the "depressed" beam of the (L. W. Taylor), 65.
Moving film, the problem of motion picture projection from continuously (Fordyce Tuttle and Chas. D. Reid), 39.
Munsell colors, standardization of (I. H. Godlove), 429-A.

N

NICHOLS, E. L. and MARY A. EWER: Thermal behavior of certain solid solutions, 456.
——— and H. L. HOWES: On temperature crests in cando-luminescence, 170.
——— and FRANCES G. WICK: The relation between certain types of luminescence, 15-A, 357.

O

Obituaries:
Lomb, Adolph, 663.
Priest, Irwin G., 503.
Troland, Leonard Thompson, 509.
O'BRIEN, BRIAN: A null method of photographic spectrophotometry with a spiral aperture sector disk, 426-A.
———, A photo-cell filter combination with spectral sensitivity approximating the visibility function, 427-A.
———, Reflection from finely crushed semi-transparent material, 9-A.
———, and F. M. E. HOLMES: Transmission of light by fog and haze, 9-A.
O'BRYAN, H. M.: Absorption and dispersion of celluloid between 300A and 1000A, 739.
Ocular images, corresponding retinal points, the horopter and size and shape of, Part I (A. Ames, Jr., Kenneth N. Ogle and Gordon H. Gliddon), 538: Part II, 575.
Officers, election of (for 1932–33), 3.
OGLE, KENNETH N., A. AMES, JR., and GORDON H. GLIDDON: Corresponding retinal points, the horopter and size and shape of ocular images. Part I, 538, Part II, 575.
OGLE, KENNETH N.: An analytical treatment of the longitudinal horopter; its measurement and application to related phenomena, especially to the relative size and shape of the ocular images, 665.
OLDENBERG, O.: On the intensity of illumination in spectrographs, 441.
Optical control, a bolometer for automatic (K. Hickman and C. R. Sanford), 13-A.
——— problems of the motion picture industry, 2.
——— properties of glass, relation between the composition and the density and. I. The soda-lime-silica glasses (G. W. Morey and H. E. Merwin), 632.

Optical Society of America. Cambridge meeting, 422.
———, proceedings of the annual meeting of the, 1.
Orthostereoscopic pictures at magnifications from unity to 24×, a camera and stereoscope for (H. F. Kurtz), 18-A.
Oscillating quartz plate, an interferometer method of studying the vibrations of an (Harold Osterberg), 19.
OSTERBERG, HAROLD: An interferometer method of studying the vibrations of an oscillating quartz plate, 19.

P

Papers in the Journal, charge for, 425.
Path length through a lens in terms of its reciprocal spherical aberration, differences in (Harold F. Bennett), 14-A.
Penetration of daylight into the sea (E. O. Hulburt), 408.
Perkins observatory reflector, optical tests of the 69-inch (Harlan T. Stetson), 432-A.
PFUND, A. H.: A universal spectrometer for the infrared, 281.
Photo-cell filter combination with spectral sensitivity approximating the visibility function (Brian O'Brien), 427-A.
Photoelasticity, new developments in (Arshag G. Solakian), 293.
Photoelectric cells, the application of, to photometry and colorimetry (Arthur C. Hardy and O. W. Pineo), 427-A.
Photoflash lamp or other source of short duration, a method of measuring the maximum intensity of light of the (W. E. Forsythe and M. A. Easley), 6-A.
Photographic lenses, a new bench for testing (R. Kingslake), 13-A, 207.
——— plates for use in spectroscopy (C. E. Mees), 17-A.
——— plates for use in spectroscopy and astronomy II. (C. E. K. Mees), 204, 427-A.
——— plates to wave lengths below 2500A, the sensitization of ordinary (A. J. Allen and R. G. Franklin), 469.
——— spectrophotometry with a spiral aperture sector disk, a null method of (Brian O'Brien), 426-A.
——— standards of intensity, report of committee on, 16.
Photography, infrared spectrum (W. F. Meggers, C. C. Kiess and C. J. Humphreys) 428-A.
———, polychrome (Frederic E. Ives), 199.
Photometric standards based on a black body at the freezing point of iridium (F. R. Caldwell, Wm. F. Roeser and L. E. Barbrow), 7-A.
——— standards, progress toward international agreement on (E. C. Crittenden), 433-A.
Photometry, applications to, of a black body immersed in freezing iridium (H. T. Wensel), 433-A.
——— and colorimetry, the applicability of photoelectric cells to, (Arthur C. Hardy and O. W. Pineo), 427-A.
PINEO, O. W. and ARTHUR C. HARDY: The applicability of photoelectric cells to photometry and colorimetry, 427-A.
———, The computation of trichromatic excitation values by the selected ordinate method, 430-A.
Plane waves of light III (Thornton C. Fry), 307, 434-A.
POINDEXTER, FRANKLIN E. and LOUIS E. JAMES: Effect of intensity and underlying fogs on the latent image, 525.
Polychrome photography (Frederic E. Ives), 199.
Priest, Irwin G., Memorial, 503.
PRIEST, IRWIN G.: Report on the work of the colorimetry committee of the international commission on illumination and the actions taken at the meeting in Cambridge, England, September, 1931, 431-A.
Proceedings of the sixteenth annual meeting 1.
Projection in relief and color (H. E. Ives), 17-A, 191.
"Properties of matter," joint symposium, (title only), 423.
Pupillary width, accommodation, and stimulus distance (Ellis Freeman), 729.
Pupillometer, a modified broca (Frank K. Moss), 735.

R

RASHEVSKY, N. P.: Some practical applications of electronic devices, (title only), 423.
Reciprocal spherical aberration, differences in path length through a lens in terms of its (Harold F. Bennett), 14-A.
Rectifying cameras, 144.
REESE, H. M.: The use of plane transmission gratings, 496.
Reflection-factors in the ultraviolet, the measurement of (A. H. Taylor), 8-A.
Reflection from finely crushed semitransparent material (Brian O'Brien), 9-A.
Refraction in the regular system, Lorentz double (E. U. Condon and F. Seitz), 393.
Regular membership, transfers from associate to, 6.
REID, CHAS. D. and FORDYCE TUTTLE: The problem of motion picture projection from continuously moving film, 39.
Relief and color, projection in (H. E. Ives), 17-A, 191.
Retinal chromatic fields as a function of wave length (Charles A. Rinde), 333.
——— points, the horopter and size and shape of ocular images, corresponding, Part I (A. Ames, Jr., Kenneth N. Ogle and Gordon H. Gliddon), 538, Part II, 575.

The Review of Scientific Instruments, statement of cash receipts and disbursements, 435.

Reviews (book):

Spectroskopie Der Roentgenstrahlen. Manne Siegbahn, 36.

Opticks, or a Treatise on the Reflections, Refractions, Inflections, and Colours of Light. Sir Isaac Newton, 36.

Seeing, A Partnership of Lighting and Vision. M. Luckiesch, 38.

Traite de Telemetrie. Capitaine P. Mazuir, 109.

Foundation and Methods of Chemical Analysis by the Emission Spectrum. Walther Gerlach and Eugen Schweitzer, 109.

The Practice of Spectrum Analysis with Hilger Instruments. Compiled by F. Twyman, 110.

L'Atome de Bohr. La Mechanique Analytique et les Quanta, Les Spectres de Multiplets. Leon Brillouin, 190.

Ultraviolet Rays and Works of Art. James J. Rorimer, 264.

Wave-length Tables for Spectrum Analysis F. Twyman and D. M. Smith, 388.

Photoelectric Phenomena. Arthur Llewelyn Hughes and Lee Alvin DuBridge, 388.

Science in Action. Edward R. Weidlein and William A. Hamor, 390.

Slit-Lamp Microscopy of the Living Eye. Dr. F. Ed. Koby, 392.

S.M.P.E. Committee Reports Recommendations for 16MM Film Standards, 436.

Photoelasticity. Coker and Filon, 436.

Atombau und Spetrallinien, Vol. I. Arnold Sommerfeld, 437.

Strahlenoptik. Dr. M. Herzberger, 438.

Optische Abbildung, Einführung in die Wellen- und Beugungstheorie optischer Systems. Dr. Johannes Picht, 438.

Motion Picture Museum, 439.

Photogrommetrie und Luftbildwesen. R. Hugershoff, 466.

The Microscope. Simon Henry Gage, 499.

Vision and Colour Vision. R. A. Houstoun, 499.

The White Dwarf Stars. E. A. Milne, 502.

Tables of Cubic Crystal Structure. I. E. Knapp, B. Karlik and C. F. Elan.

RINDE, CHARLES A.: Retinal chromatic fields as a function of wave length, 333.

ROCKWOOD, R. S. and R. A. SAWYER: Ultraviolet transmission coefficient of the earth's atmosphere, 513.

ROESER, WM. F., L. E. BARBROW and F. R. CALDWELL: Photometric standards based on a black body at the freezing point of iridium, 7-A.

S

SANFORD, C. R. and K. HICKMAN: A bolometer for automatic optical control, 13-A.

SAWYER, R. A. and R. S. ROCKWOOD: Ultraviolet transmission coefficient of the earth's atmosphere, 513.

Schumann plates, a simplified method of preparing (J. J. Hopfield and E. T. S. Appleyard), 488.

Sea, on the penetration of daylight into the (E. O. Hulburt), 408.

Secretary's report for 1931, 236.

SEITZ, F. and E. U. CONDON: Lorentz double refraction in the regular system, 393.

Semitransparent material, reflection from finely crushed (Brian O'Brien), 9-A.

Sensibility to temperature change as a function of color temperature, choromaticity (Deane B. Judd), 9-A.

Sensitization of ordinary photographic plates to wave lengths below 2500A (A. J. Allen and R. G. Franklin), 469.

SILBERSTEIN, LUDWIK: Determination of the spectral composition of x-ray radiation from filtration data, 265.

Silicates, crystal structure of the (B. E. Warren) (title only), 423-A.

Sin x/x, the function of (Simon H. Bauer), 537.

SLEATOR, W. W.: The elliptic polarization of light by total internal reflection, 15-A.

SMYTH, C. P.: Molecular shape and orientation of liquids, (title only), 423-A.

Soda-lime-silica glasses, I. Relation between the composition and the density and optical properties of glass. (G. W. Morey and H. E. Merwin), 632.

SOLAKIAN, ARSHAG G.: New developments in photoelasticity—a purely optical method of stress analysis, 293.

Solid solutions, thermal behavior of certain (E. L. Nichols and Mary A. Ewer), 456.

Spectral composition of x-ray radiation from filtration data, determination of the (Ludwik Silberstein), 265.

Spectrograms, the interpretation of (A. H. Taylor and T. Knowles), 229.

———, measuring microscope and densitometer for (Gustave Fassin), 13-A.

——— without an absorbing wedge (Oran E. Miller), 13-A.

Spectrograph, especially at large angles of incidence, on the concave grating (J. E. Mack, J. R. Stehn, and Bengt Edlén), 245.

Spectrographs, on the intensity of illumination (O. Oldenberg), 441.

Spectrometer for the infrared, a universal (A. H. Pfund), 281.

Spectrophotometry, photographic, a null method of (Brian O'Brien), 426-A.

Spectroscopy and astronomy II, photographic plates for use in (C. E. Kenneth Mees), 204, 427-A.

Spectroscopy, photographic plates for use in (C. E. K. Mees), 17-A.
Spherical aberration, differences in path length through a lens in terms of its reciprocal (Harold F. Bennett), 14-A.
——— surfaces of small curvature, an attachment for producing approximately, on a lathe (I. C. Gardner), 432-A.
STEHN, J. R., J. E. MACK, and BENGT EDLÉN: on the concave grating spectrograph, especially at large angles of incidence, 245.
Stereo-photographic mapping instruments and methods, aerial (C. H. Birdseye), 137.
Stereoscope for orthosteroscopic pictures at magnifications from unity to 24×, a camera and (H. F. Kurtz), 18-A.
STETSON, HARLAN T.: Optical tests of the 69-inch Perkins Observatory reflector, 432-A.
Stimulus differences, chromaticity sensibility to (Deane B. Judd), 72.
——— distance, accommodation and pupillary width (Ellis Freeman), 729.
———, anomalies of visual acuity in relation to (Ellis Freeman), 285.
———, intensity area, and distance of visual (Ellis Freeman), 402.
STOKLEY, JAMES: An eclipse projector for the Franklin Institute museum, 239.
Stratton, S. W., Tribute to, 2.
Surface polish upon the light transmitted in "total" reflexion, the influence of (Armand de Gramont), 11-A.

T

TAYLOR, A. H.: The measurement of reflection-factors in the ultraviolet, 8-A.
——— and T. KNOWLES: The interpretation of spectrograms, 229.
TAYLOR, L. W.: The "depressed" beam of the motor car headlight, 65.
Testing photographic lenses, a new bench for (R. Kingslake), 13-A, 207.
Thermal behavior of certain solid solutions (E. L. Nichols and Mary A. Ewer), 456.
"Total" reflexion, the influence of surface polish upon the light transmitted in (Armand de Gramont), 11-A.
Transmission gratings, the use of plane (H. M. Reese), 496.
——— of light by fog and haze (F. M. E. Holmes and Brian O'Brien), 9-A.
Treasurer's report for 1931, 749.
Trichromatic colorimeter, a (J. Zernike), 418.
———, excitation values, the computation of, by the selected ordinate method (Arthur C. Hardy and O. W. Pineo), 430-A.
———, functions of the average eye (W. F. Hamilton and Ellis Freeman), 369.
Troland, Leonard Thompson, Memorial, 509.
TUTTLE, FORDYCE and CHAS. D. REID: The problem of motion picture projection from continuously moving film, 39.

U

Ultraviolet, the measurement of reflection-factors in the (A. H. Taylor), 8-A.
———, rays on pharmacological potency of digitalis, influence of (David I. Macht), 16-A.
———, transmission coefficient of the earth's atmosphere (R. S. Rockwood and R. A. Sawyer), 513.
Universal spectrometer for the infrared, a (A. H. Pfund), 281.

V

VERNON, ARTHUR A. and GORTON R. FONDA: Characteristics of coiled filaments in incandescent lamps, 223.
Visibility function, a photocell filter combination with spectral sensitivity approximating the (Brian O'Brien), 427-A.
Visual acuity in relation to stimulus-distance, anomalies of (Ellis Freeman), 285.
——— stimulus, intensity, area, and distance of (Ellis Freeman), 402.
Voltages, special tubes for the amplification of small (G. F. Metcalf) (title only), 423.

W

WARREN, B. E.: Crystal structure of the silicates (title only), 423-A.
Wave length, retinal chromatic fields as a function of (Charles A. Rinde), 333.
Waves, plane, of light. III: Absorption by metals (T. C. Fry), 307, 434-A.
Wedge spectrograms without an absorbing wedge (Oran E. Miller), 13-A.
WENSEL, H. T.: Applications to photometry of a black body immersed in freezing iridium, 433-A.
——— and F. HENNING: The freezing point of iridium, 7-A.
Wetzel, Reinhard A.: Photographs of the Lummer "doubling" of interference fringes of equal slope in polarized light, 14-A.
WICK, FRANCES G. and E. L. NICHOLS: The relation between certain types of luminescence, 15-A, 357.

X

X-ray radiation from filtration data, determination of the spectral composition of (Ludwik Silberstein), 265.

Z

ZERNIKE, J.: Trichromatic colorimeter, 418.